

Università degli Studi di Milano
Dipartimento di Medicina, Chirurgia e Odontoiatria
Laboratori di Farmacologia, Polo Universitario S. Paolo



Dottorato di Ricerca in
Fisiopatologia, Farmacologia, Clinica e Terapia
delle Malattie Metaboliche (XXIII ciclo)

***NEW NON SYNTHETIC MOLECULES ARE ABLE
TO INHIBIT APOPTOSIS IN DERMAL PAPILLAR
CELLS OF HAIR BULBS***

Settore scientifico disciplinare: **BIO-14**

Coordinatore del Corso di Dottorato: **Chiar.ma Prof.ssa A.M. Di Giulio**

Docente Guida: **Chiar.mo Prof. A. Gorio**

Tesi di dottorato di: **Traversa Maria Vittoria**

Matr. n°R07662

Anno accademico 2009-2010

*A mia madre,
...Non ci sono parole
per descriverti...*

Index

Summary	pag.05
1.Introduction	pag.07
1.1 Hair Follicle	
1.2 Androgenetic alopecia	
1.3 Apoptosis	
1.3.1 <i>Apoptotic signalling: basic principles</i>	
1.3.2 <i>Apoptotic cell remodelling</i>	
1.4 EDA/EDAR Signaling Pathways in Hair Follicle Induction	
1.5 Wnt/DKK1	
1.6 Akt and ERK kinases	
1.7 Non synthetic molecules	
1.7.1 <i>Rutin</i>	
1.7.2 <i>Spermidine</i>	
1.7.3 <i>Zeaxanthin</i>	
1.7.4 <i>Epigallocatechin gallate</i>	
2.Aim	pag.38
3.Materials and Methods	pag.41
3.1 HFDP cells culture	
3.2 Protein quantification	
3.3 RNA and Protein extraction	
3.3.1 <i>RNA extraction</i>	
3.3.2 <i>Protein extraction</i>	
3.4 SDS Page, Western blotting and protein detection	
3.4.1 <i>Protein sample preparation for electrophoresis</i>	
3.4.2 <i>SDS Page</i>	
3.4.3 <i>Western blotting and protein detection</i>	
3.5 Caspase-3 activity	
3.6 Confocal microscopy	
<i>Specimen Preparation and Imaging</i>	
<i>Critical aspects of Confocal microscopy</i>	

3.6.1 <i>Cell culture immunofluorescence</i>	
3.7 Tunel Assay	
3.7.1 <i>Apoptosis Detenction</i>	
3.8 <i>Prevention of protein degradation in ex-vivo hair bulbs</i>	
3.9 <i>Statistical Analysis</i>	
3.10 <i>Materials</i>	
4.Result.....	pag.70
4.1 <i>Anti-apototic effect of compounds under investigation</i>	
4.2 <i>Morphological and biochemical evaluation of the anti-apoptotic action of the three active principles</i>	
4.3 <i>Investigation of EDA-A1/EDAR expression</i>	
4.4 <i>TUNEL assay</i>	
4.5 <i>HFDP cells proliferation</i>	
4.6 <i>Prevention of protein degradation in ex-vivo hair</i>	
5.Discussion.....	pag.94
6. Bibliography.....	pag.99

Summary

Hair exerts a range of functions including thermoregulation, physical protection, sensory activity. Mature and actively growing hair follicles become anchored in the subcutis, and regenerate by spontaneous repetitive cycles of growth (anagen), apoptosis-driven regression (catagen), and quiescence (telogen). We focused our study on investigating the effect of new therapeutic molecules capable of counteracting the regression phase. We have tested our working hypothesis on HFDPC cells, grown in culture in Follicle Dermal Papilla Growth Medium, and apoptosis was induced by 24 hours incubation with 1 μ M staurosporin. This treatment resulted in a marked activation of Caspase-3 accompanied by cytoskeletal degradation, nuclear blebbing, and cellular fragmentation. The addition of spermidin or rutine in the micromolar range concentration reduced staurosporin-induced caspase activity by over 50%, when the two agents were added simultaneously equal levels of caspase-3 inhibition was achieved with concentration 10 fold lower. Zeaxantine alone was ineffective, however when added to the combined spermidin and rutine treatment, the staurosporin-induced caspase activity was almost totally counteracted and the enzymatic activity was significantly reduced. These combined treatment was also effective in preventing staurosporin-mediated cellular damage. The extent of cell loss was greatly reduced and there was a total preservation and normal distribution of actin-tubulin cytoskeleton with normal cellular shape. Interestingly, our combined treatment also counteracted caspase-3 over-expression induced by staurosporin. In conclusion, this spermidin and rutine can counteract HFDPC cells apoptosis and may represent an effective preventing treatment for the catagen phase of the hair bulb life cycle.

1. Introduction

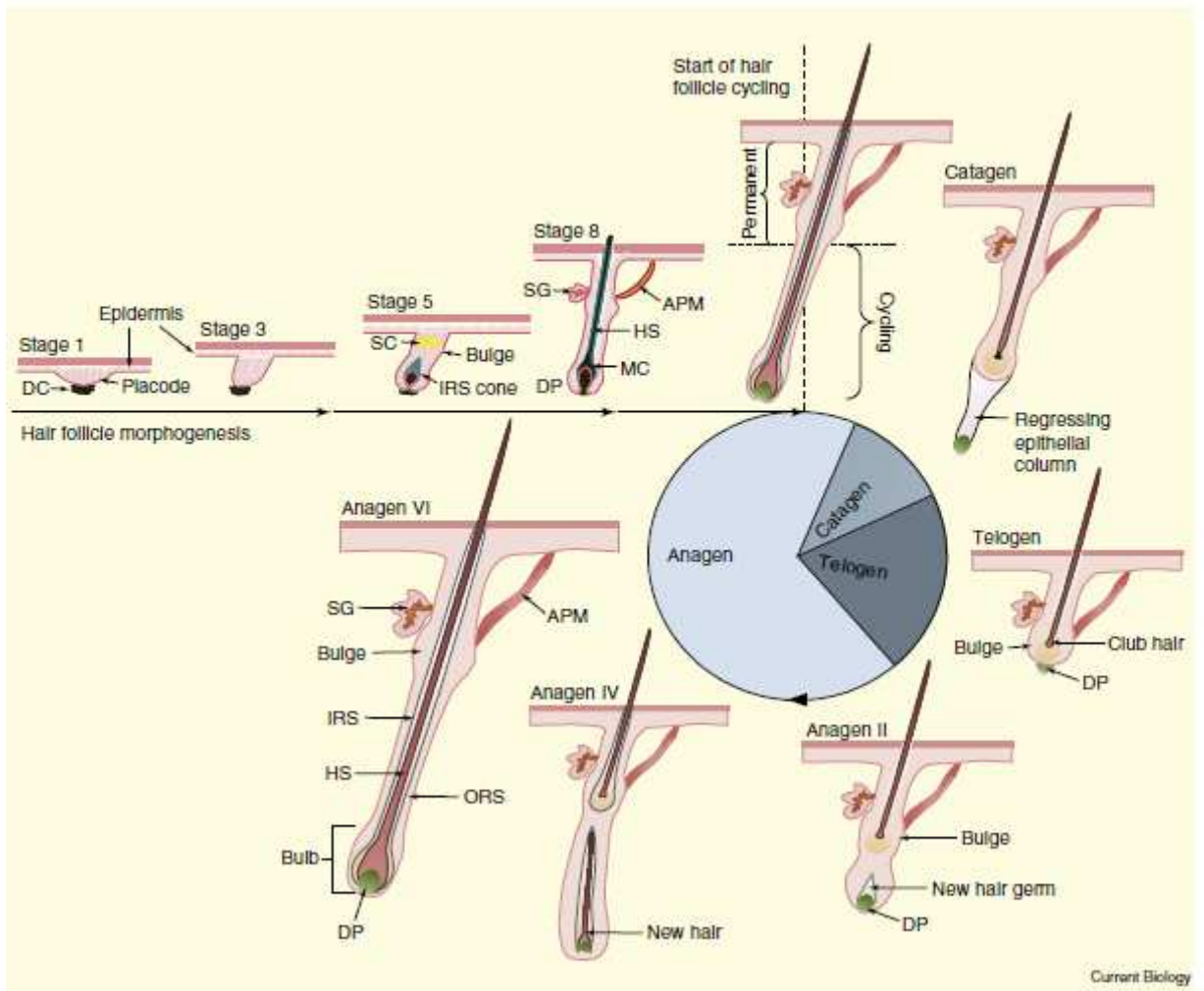
1.1 Hair Follicle

The hair follicle (HF) is located in the dermis and subcutaneous tissue. It is a skin appendage with complex structure and functions, formed by an indentation of epithelium [Weinberg et al.]. It is considered one of the most important model for study on development and regeneration of tissues and organs, as it has a comparatively small size and has the characteristics of self-renewal and cycling growth [Gambarella et al.; Brouard et al.; Trueb].

Dermal papilla cells (DPCs) are a group of dermal cells located in the bulbar zone of HF. They are a group of specific fibroblasts that represent a main component in the mesenchyma of HF, and play a leading role in regulating the development and cycling regeneration of HFs [Roh et al.; Botchkarev et al.; Rendl et al.]. During the initial stage of HF morphogenesis, DPCs can self-aggregate in the dermis and induce an epidermal placode (an area of thickening in the embryonic epithelial layer where an organ or structure later develops) to form follicular structures [Stenn et al.; Millar]. DPCs are mesenchymal cells, and can thus differentiate into a variety of cell types, and they have been shown to induce neogenesis of HFs in hairless skin [Osada et al.; McElwee et al.]. It should be noted that the ability of DPCs to induce HF formation depends on their aggregative growth; defined as a multiradial growth phenomenon occurring before fusion of DPCs, and is a defining characteristic of DPCs that are able to induce HF formation. DPCs that grow in an aggregative manner are polygonal, with multiple protuberances, and are arranged in a radial pattern.

A hair follicle (HF) cycles through anagen (growth), catagen (involution) and telogen (resting) phases, and then re-enters the anagen phase (Figure 1). Each hair passes through the phases independent of the neighbouring hairs [Matsusaki et al.]

Approximately 85% of all hairs are in the growing phase at any one time. The Anagen phase, or growth phase, can vary from two to six years. Hair grows approximately 10cm per year and any individual hair is unlikely to grow more than one meter long. At the end of the Anagen phase the hairs enters into a Catagen phase which lasts about one or two weeks, during the Catagen phase the hair follicle shrinks to about 1/6 of the normal length. The lower part is destroyed and the dermal papilla breaks away to rest below. The resting phase follows the catagen phase and normally lasts about 5-6 weeks. During this time the hair does not grow but stays attached to the follicle while the dermal papilla stays in a resting phase below. Approximately 10-15 percent of all hairs are in this phase at an one time. At the end of the Telogen phase the hair follicle re-enters the Anagen phase. The dermal papilla and the base of the follicle join together again and a new hair begins to form. If the old hair has not already been shed the new hair pushes the old one out and the growth cycle starts all over again.

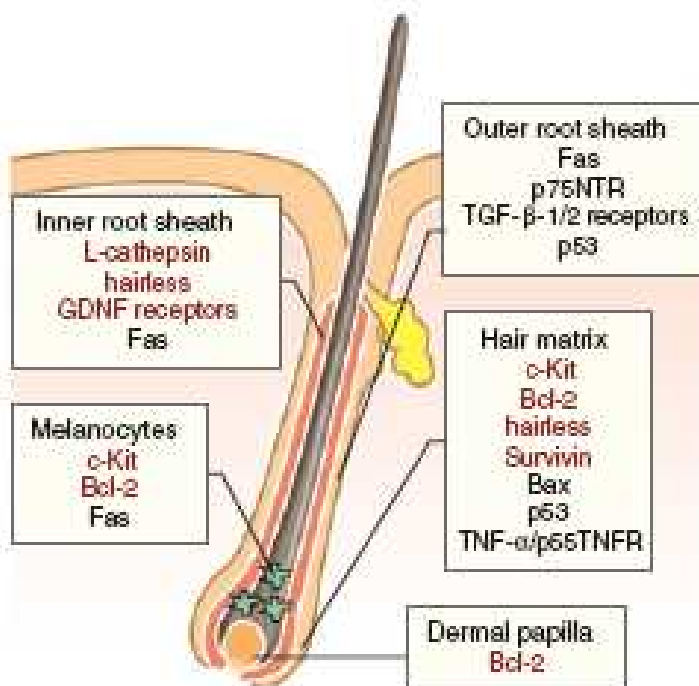


[from: Marlon R. Schneider et al 2009 Current Biology 19, R132–R142]

Figure 1. Key stages of the hair cycle.

The hair cycle is divided into three phases: Anagen (growth phase), catagen (regression phase) and telogen (resting phase). Postnatal hair morphogenesis leads to elongation of the follicle and production of the hair fibre, which emerges from the skin. Once the hair follicle has matured, it enters the regression phase, during which the lower, cycling portion of the hair follicle is degraded. This process brings the dermal papilla into close proximity of the bulge, where the hair stem cells (HSCs) reside. The molecular interaction between the HSCs and the dermal papilla is essential to form a new hair follicle. The proximity between bulge and dermal papilla is maintained throughout telogen, the resting phase. Only when a critical concentration of hair growth activating signals is reached, anagen phase is entered and a new hair is re-grown. The first postnatal hair cycle is initiated and passed by all hair follicles at the same time point, while subsequent cycles are no longer synchronized. Stages 1–8 of embryonic hair development are depicted (upper left), demonstrating the continuous transition between hair follicle development and the first postnatal hair cycle. APM: arrector pili muscle; DC, dermal condensate (green); DP: dermal papilla (green); HS: hair shaft (brown); IRS: inner root sheath (blue); MC: melanocytes; ORS: outer root sheath; SC: sebocytes (yellow); SG: sebaceous gland.

At the base of this cycle is the ability of HF stem cells to briefly exit their quiescent status to generate transient amplifying progeny [Kligman]. It seems that, within a single hair follicle, periodic activation of beta-catenin in bulge stem cells is responsible for their cyclic activity. During HF growth and hair production, the activity of factors promoting the proliferation, differentiation and survival predominates. HF regression, or catagen, is characterized by activation of pathways that induce apoptosis in HF cells (Figure 2). Data Obtained from murine and human HF suggest that apoptosis could be controlled both by extrinsic and intrinsic pathways [Schneider et al.].



[from: Botchkareva et al. (2006) J Inv. Dermatol. 126: 258-64]

Fig. 2 Anti- and pro-apoptotic molecules expressed in distinct hair follicle compartments

Distinct cell populations in the HF possess differential susceptibility to apoptosis. The most susceptible to apoptosis are the majority of the follicular epithelial cells and melanocytes, whereas dermal papilla fibroblasts, some of the keratinocytes and melanocytes selected for survival, are resistant to apoptosis. HF development and cycling are controlled by similar signalling networks within and between the follicular epithelium and mesenchyme, using the molecules that belong to the bone morphogenetic protein (BMP)/TGF-beta, EGF, FGF, IGF, neurotrophin, TNF, and Wnt families [Langbein et al.]. Recent studies suggest regulation of HF homeostasis by dermal papillar cells through the autocrine and paracrine production of specific factors, from which an important role is attributed to a Dkk family proteins [Kwack et al.]. The exposure of dermal papillar cells to dihydrotestosterone determines the up-regulation of DKK1, that is then secreted thereby triggering the apoptosis of outer root sheath keratinocytes. Differently the expression of IGF-1 by follicular dermal papillar cells is promoted by finasteride treatment of androgenic alopecia [Wakisaka et al.; Weger et al.].

1.2 Androgenetic alopecia

Androgenetic alopecia is a common form of hair loss in both men and women. In men, this condition is also known as male-pattern baldness. Hair is lost in a well-defined pattern, beginning above both temples. Over time, the hairline recedes to form a characteristic "M" shape. Hair also thins at the crown (near

the top of the head), often progressing to partial or complete baldness [Muller; Hamilton].

The pattern of hair loss in women differs from male-pattern baldness. In women, the hair becomes thinner all over the head, and the hairline does not recede. Androgenetic alopecia in women rarely leads to total baldness.

Androgenetic alopecia in men has been associated with several other medical conditions including coronary heart disease and enlargement of the prostate [Lesko et al.]. Additionally, prostate cancer, disorders of insulin resistance (such as diabetes and obesity), and high blood pressure (hypertension) have been related to androgenetic alopecia [Ellis et al.; Oh et al.; Hawk et al.; Ahouansou et al.]. In women, androgenetic alopecia is associated with an increased risk of polycystic ovary syndrome (PCOS). PCOS is characterized by a hormonal imbalance that can lead to irregular menstruation, acne, excess body hair (hirsutism), and weight gain [Rathnayake et al.].

Although androgenetic alopecia is a frequent cause of hair loss in both men and women, it is more common in men. This form of hair loss affects an estimated 35 million men in the United States. Androgenetic alopecia can start as early as a person's teens and risk increases with age; more than 50 percent of men over age 50 have some degree of hair loss. In women, hair loss is most likely after menopause [Ludwig].

A variety of genetic and environmental factors likely play a role in causing androgenetic alopecia. Although researchers are studying risk factors that may contribute to this condition, most of these factors remain unknown. Researchers have determined that this form of hair loss is related to androgens hormones, particularly dihydrotestosterone. Androgens are

important for normal male sexual development before birth and during puberty [Kaufman] .

Androgens also have other important functions in both males and females, such as regulating hair growth and sex drive.

Hair growth begins under the skin in the follicles. Each strand of hair normally grows for 2 to 6 years, goes into a resting phase for several months, and then falls out. The cycle starts over when the follicle begins growing a new hair. Increased levels of androgens in hair follicles can lead to a shorter cycle of hair growth and the growth of shorter and thinner strands of hair. Additionally, there is a delay in the growth of new hair to replace strands that are shed [Olsen].

Although researchers suspect that several genes play a role in androgenetic alopecia, variations in only one gene, AR, have been identified in people with this condition. The AR gene provides instructions for making androgen receptor. Androgen receptor is the intracellular protein that mediates biological actions of physiological androgens (testosterone and 5 alpha-dihydrotestosterone). Androgen receptor belongs to a large family of ligand-dependent proteins whose function is to modulate expression of genes and gene networks in a cell- and tissue-specific manner [Janne].

Androgen receptors allow the body to respond appropriately to dihydrotestosterone and other androgens. Studies suggest that variations in the AR gene lead to increased activity of androgen receptors in hair follicles. It remains unclear, however, how these genetic changes increase the risk of patterned hair loss in men and women with androgenetic alopecia.

Researchers continue to investigate the connection between androgenetic alopecia and other medical conditions, such as coronary heart disease and

prostate cancer in men and polycystic ovary syndrome in women. They believe that some of these disorders may be associated with elevated androgen levels, which may help explain why they tend to occur with androgen-related hair loss. Other hormonal, environmental, and genetic factors that have not been identified also may be involved [Hawk] .

The inheritance pattern of androgenetic alopecia is unclear because many genetic and environmental factors are likely to be involved. This condition tends to cluster in families, however, and having a close relative with patterned hair loss appears to be a risk factor for developing the condition [Muller;Hamilton].

1.3 Apoptosis

Apoptosis is a common mechanism among multicellular organisms to eliminate cells that are no longer needed or have become damaged. It is a morphologically and biochemically distinct form of cell death that can be triggered by a wide range of internal and external signals.

It occurs in response to environmental or developmental cues, cellular stresses, and specific cell death signals. This self-inflicted death, named for a characteristic rounding and “falling off” of cells, involves a number of evolutionarily conserved biochemical pathways that have been intensively studied for over two decades [Taylor et al.]. Apoptotic cell death is generally characterized by an inward collapse of organelles, a “blebbing” of the plasma membrane into vesicular apoptotic bodies, and the destruction of genetic material [Ferri et al.]. The molecular events regulating apoptosis are dependent

on cell type as well as the context of death induction. Nonetheless, key molecular milestones are common to many of modes of cell death. Apoptosis is essential during the development of multicellular organisms [Kuida et al.]. It also eradicates damaged or virally infected cells throughout the life of an organism in the absence of an inflammatory response [Savill et al.]. It does this by engaging a series of coordinated changes in cell structure/behaviour that culminate in the presentation of surface markers that flag the dying cell for engulfment by professional or non-professional phagocytes [Savill et al.]. For this to occur, dying cells must retain the capacity to control the organisation/positioning of membranes and proteins long enough to bring about their recognition by phagocytes. Most observers consider the execution phase of apoptosis - the time during which gross apoptotic morphological/behaviour changes are observed and before the cell begins the process of secondary necrosis - to last for around 1-2 hours [Mills et al.; Moss et al.]. Hence, a dying cell has a limited time window during which it must coordinate both the changes in morphology that are required for its isolation and the exposure of novel and/or altered surface moieties that are needed for efficient recognition and engulfment.

1.3.1 Apoptotic signalling: basic principles

Apoptosis can be induced by an array of toxic insults, physiological and non-physiological, which all converge on the activation of a family of proteases called caspases [Earnshaw et al.; Fan et al.]. These enzymes are present in the cytosol of all viable cells as zymogens with low intrinsic activity, providing

cells with the capability to rapidly trigger apoptotic protease action without the need for new protein synthesis. Apoptotic caspases fall into two general classes: the initiator caspases that are required for initial apoptotic signalling and the executioner caspases whose roles are to cleave a variety of important structural and regulatory proteins at conserved aspartic acid residues to alter their functions irreversibly [Earnshaw et al.; Taylor et al.]. Members of the Bcl-2 family of pro- and anti-apoptotic signalling molecules integrate these signals, and their interactions dictate whether or not a cell enters the apoptotic execution phase. Importantly, many of these are known to associate with organelles of the endomembrane system or with cytoskeletal components [Betin et al.]. Of particular importance are the interactions between Bcl-2 family members and the mitochondria which harbour an array of apoptotic signalling molecules whose release via Bcl-2 family engagement triggers a robust apoptotic response; although relationships between Bcl-2 family members and the endoplasmic reticulum (ER) are also significant particularly with respect to calcium signalling or in cells subject to oxidative stress [Ferri et al.]. Induction of mitochondrial outer membrane permeabilisation (MOMP) via Bcl-2 family members causes release of cytochrome c, which, in turn, activates the initiator caspase-9 by inducing assembly of the “apoptosome” - a complex consisting of multiple copies of caspase-9, cytochrome c, dATP and the adaptor APAF-1. Caspase-9, in turn, activates effector caspases that cleave target proteins to initiate the apoptotic execution phase proper. Mitochondria are therefore central to a cell’s apoptotic response. The other major mechanism for activating caspases in response to death stimuli is via cell surface engagement of death receptors such as those of the TNF family (e.g. Fas receptor/CD95). Death

receptors can activate caspases directly, or via mitochondrial amplification. As transmembrane proteins that exert their influence at the plasma membrane, their trafficking through the secretory and endocytic systems is a key feature of death receptor signalling. It has become apparent that both the secretory and endocytic systems are disrupted as an early consequence of caspase activation, but it is unclear how this impacts upon death receptor distribution, trafficking and signalling “Executioner” caspases such as caspase-3 carry out the final, committed steps of the apoptotic program after activation of upstream, apical “initiator” caspases, such as caspase-8, which activate apoptosis through two generalized pathways (Figure 3). Caspase-3 (also known as CPP32, Yama or apopain) is the most important apoptosis effector. In quiescent conditions caspase-3 is inactive (pro-enzyme), following pro-apoptotic stimuli it becomes processed and activated by caspases-8 and-9.

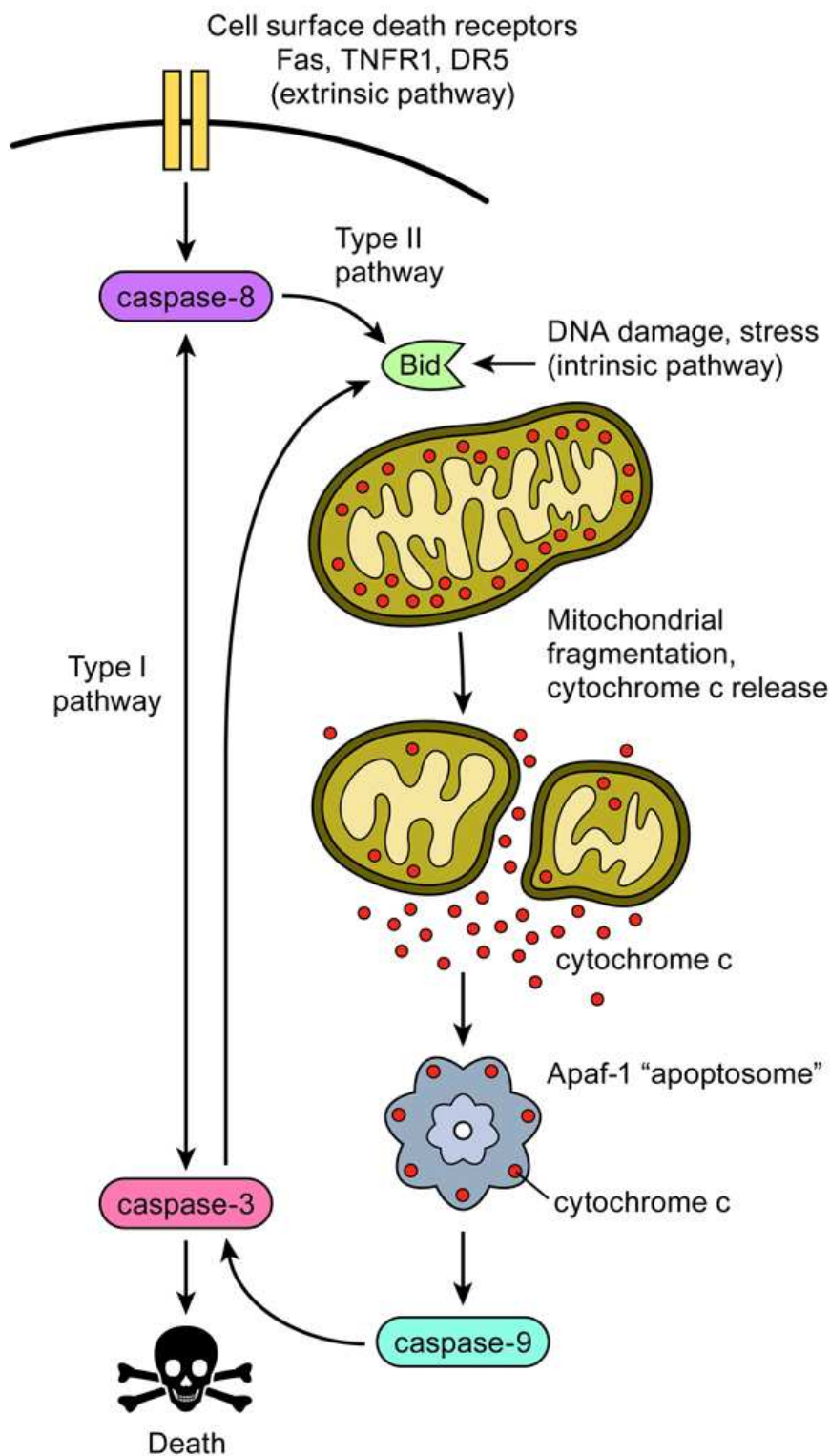


Figure 3. Essential pathways to caspase activation and cell death

Apoptosis is initiated by internal cellular stress or extracellularly through the binding of ligands to cell surface death receptors. Type I pathways directly activate executioner caspases through initiator caspases to result in death. In Type II pathways, death signals are routed through the Bcl-2 proteins such as Bid and the mitochondria to control the release of cytochrome c. Cytosolic cytochrome c binds Apaf-1 to activate the apoptosome and caspase-9 to result in executioner caspase-3 activation and cell death.

1.3.2 Apoptotic cell remodelling

The dramatic changes in cell behaviour observed during the apoptotic execution phase are orchestrated by caspases. In response to targeted protein cleavage, apoptotic cells begin a process of remodelling which includes cell retraction, plasma membrane blebbing and often fragmentation of the cell into membrane-bound apoptotic bodies. In epithelia the execution phase also invokes the actions of neighbouring cells that respond to early changes in the dying cell (possibly allied to cytoskeletal deregulation and changes in lateral tensile resistance) to initiate its extrusion [Rosenblatt et al.]. Extrusion then follows a regulated sequence of events involving the redistribution of actin and microtubule cytoskeletons within neighbouring cells to squeeze the dying cell (usually apically) via p115 RhoGEF-mediated actin contractility [Slattum et al.]. Fragmentation is also largely actin/myosin II driven [Mills et al; Moss et al.], and probably aids cell engulfment [Moss et al.] while also providing carriers for the dispersal of potent autoimmune factors [Savill et al.]. Live-cell imaging of cells treated with a variety of apoptosis inducing factors suggests that surface blebbing is one of the earliest morphological features of the execution phase [Lane et al]. Surface blebbing is a regulated process requiring caspase cleavage and activation of the Rho effector, ROCK1 and remodelling of the actin cytoskeleton (Coleman et al.; Sebbagh et al.). Its exact roles are not understood, but these may include apoptotic cell recognition, cytoplasmic mixing and energy depletion [Sebbagh et al.]. In adherent cells, blebbing and retraction begin simultaneously, although addition of myosin II inhibitors (such as blebbistatin) prevents blebbing but does not block cell retraction, suggesting that these processes are not mutually dependent [Lane et al.]. Close inspection

of adherent cells in isolation suggests that blebbing is biphasic (Fig. 1): the early blebbing phase begins concomitant with cell retraction, is characterised by numerous, small, dynamic blebs and lasts for around 40 minutes; the second phase is initiated after a brief pause, and is associated with fewer, large blebs that decorate the cell surface asymmetrically [Lane et al.]. Importantly, non-adherent cell-lines demonstrate only a single phase of blebbing, and these blebs are equivalent to the late blebs in adherent cells on account of their morphology and timing in relation to exposure of the plasma membrane inner leaflet lipid, phosphatidyl serine (PS) [Lane et al.]. These observations suggest that early blebbing is initiated during cell retraction and is restricted to adherent cell types, an important consideration when comparing the apoptotic phenotype across different cell lineages. Equally, our observations that the active redistribution of membranes and organelle fragments into surface blebs correlates with late blebbing [Lane et al.], suggest that it is this stage of remodelling that is important for the final stages of apoptotic cell partitioning and eventual disposal.

1.4 EDA/EDAR Signaling Pathways in Hair Follicle Induction

Hair follicle development requires reciprocal communication between surface epithelial cells and the underlying mesenchyme that is mediated by secreted signaling molecules. Signaling from the placodes promotes clustering of underlying dermal fibroblasts, forming dermal condensates that are the precursors of hair follicle dermal papillae. Further signaling interactions between the hair placode and the nascent dermal papilla lead to placode down-growth and hair follicle morphogenesis. Among known signaling mechanisms involved in hair follicle development, the Wnt/b-catenin and EDA/EDAR/NF- κ B pathways appear to play the earliest roles [Hammerschmid et al.].

Ectodysplasin receptor Edar and its ligand Eda A1, as well as their related receptor Xedar and ligand Eda A2, are members of the tumor necrosis factor superfamily that signal predominantly through the nuclear factor- κ B and c-jun N-terminal kinases pathways. Mutations in genes that encode proteins involved in Edar signaling pathway cause hypohidrotic ectodermal displasias in humans and mice and characterized by severe defects in development of ectodermal appendages including hairs, teeth, and exocrine glands [Cui et al.; Fessing et al.]. Expression of several Wnt ligands and Wnt reporter transgenes is specifically elevated in developing hair follicles, and forced activation of b-catenin signalling promotes hair follicle fate in both embryonic and postnatal skin. Conversely, ectopic expression of the secreted Wnt inhibitor DKK1 in embryonic mouse epidermis prevents the initiation of hair follicle development and blocks patterned expression of all molecular placode markers, including Wnt ligands, suggesting the importance of an earlier acting, broadly expressed

Wnt signal [Andl et al.]. Binding of the A1 isoform of the Tumor Necrosis Factor α (TNF α) family member Ectodysplasin (EDA) to its receptor EDAR induces nuclear translocation of the transcription factor NF- κ B, and NF- κ B pathway activation in developing hair follicle placodes [Laurikkala et al.]. Eda-A1 (391 aa) and Eda-A2 (389 aa) differ only by an insertion of two amino acids in the TNF domain due to the usage of alternative splice donor sites [Mikkola et al.]. Surprisingly, Eda-A1 and Eda-A2 were found to engage two different receptors: Edar is the specific receptor for Eda-A1 whereas X-linked Eda-A2 receptor (Xedar), another related but distinct TNFR binds Eda-A2, but not Eda-A1. Eda-A1 and Eda-A2 isoforms are trimeric proteins produced as type II transmembrane proteins with a short N-terminal intracellular domain and a fairly large C-terminal extracellular domain containing a (G-X-Y)₁₉ collagen-like repeat with one interruption followed by the TNF homology domain (see Figures 3 and 4) [Prodi et al.].

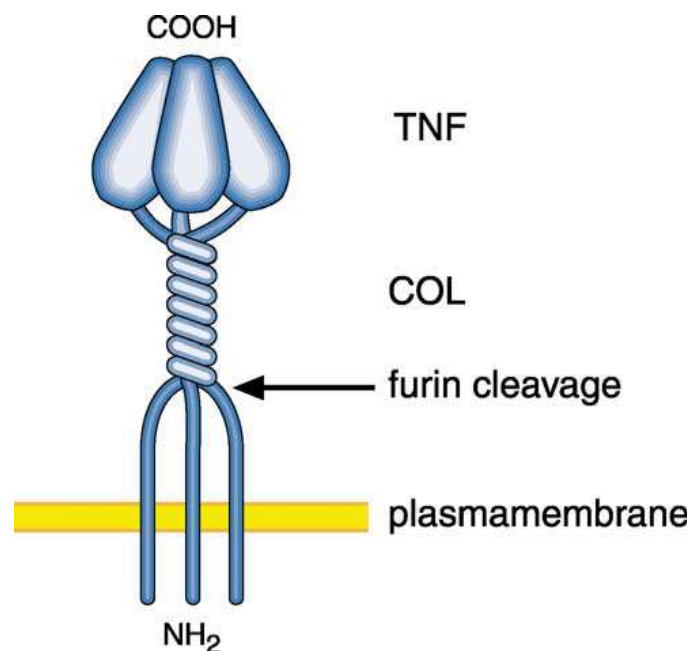


Figure 4. Schematic representation of ectodysplasin.

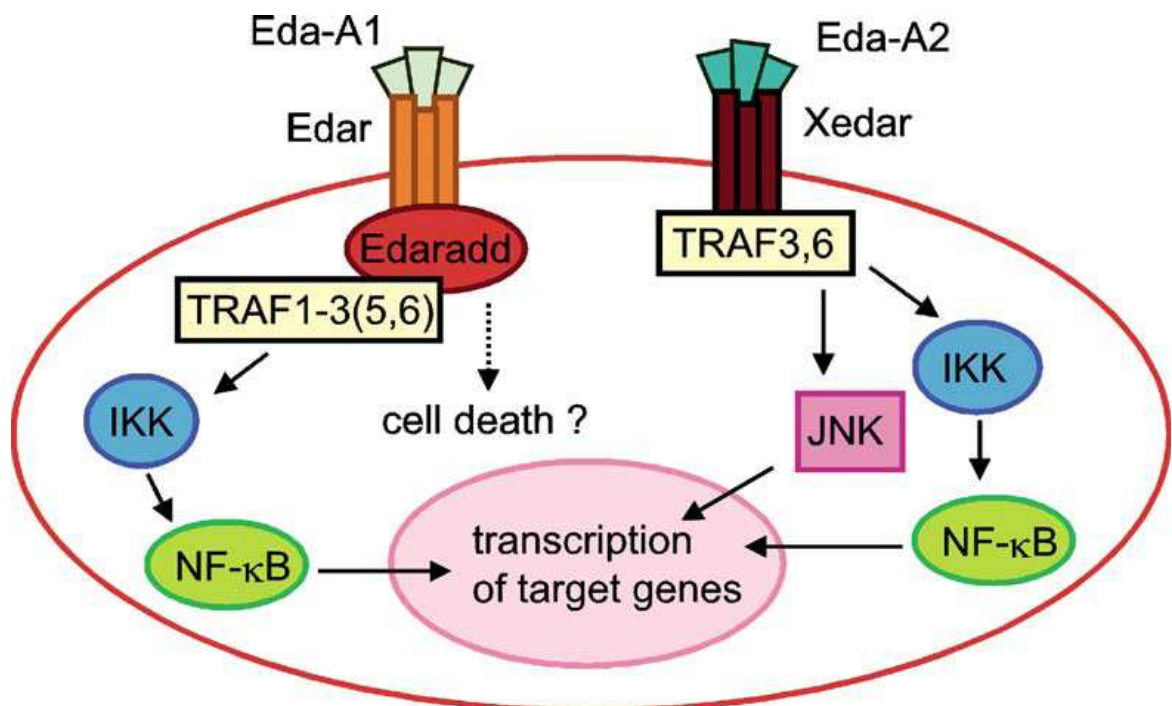


Figure 5. Summary of Edar and Xedar signal transduction pathways. Engagement of a cleaved form of Eda-A1 with Edar results in the formation of a complex containing the adapter proteins Edaradd and Traf family members leading eventually to the activation of NFK-B. Xedar is activated by Eda-A2 and can directly bind to Trafs. Traf6 is specifically required for the activation of NFK-B and JNK pathways by Xedar.

The expression of ectodysplasin and Edar has been analyzed in detail during murine hair and tooth development (Figure 6) whereas there is only one report on the expression of Xedar. In general, Eda and Edar are restricted to the ectodermal cells, and where analyzed, Edaradd has been detected in the same cells as Edar . During early development, Eda and Edar are colocalized in the simple ectodermal sheet covering the embryo. Upon initiation of tooth (E11) and hair (E14) development Edar becomes restricted to the forming placodes whereas Eda shows complementary expression in the flanking ectoderm. For most part, the analysis of Eda expression has been done by in situ hybridization, which cannot distinguish between the two isoforms. No detailed expression data of Eda is available in adults. Northern blot analysis has

revealed expression of human Eda in heart, kidney, and pancreas, as well as weaker expression in brain, placenta, lung, liver, and skeletal muscle. This correlates fairly well with the analysis done in mice. Using a more sensitive RT-PCR method, expression of Eda has been seen in practically all human tissues tested. [Midorikawa] In situ analysis shows that in adults, the expression is mainly epithelial. In addition to the affected organs, expression has been detected in kidney, sympathetic ganglia, hypothalamus, in the mammary gland epithelium, and in the duct epithelium of the prostate. The importance of the adult expression is currently not known. Expression of Eda has been studied only in few pathological situations. Its expression seems to be less abundant in both benign and malignant [Mikkola].

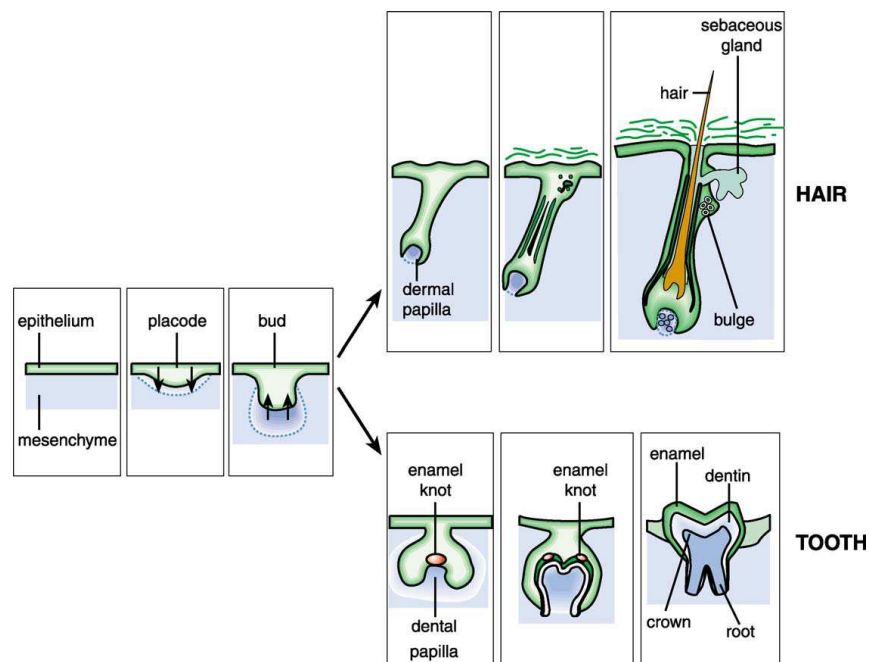


Figure 6. The development of a hair and a tooth.

Both teeth and hairs form from surface epithelium and underlying mesenchyme and their development is regulated by interactions between the two tissues. The early stages are morphologically similar as the ectodermal placodes develop, form buds and induce the formation of the dermal and dental papillae. The hair shaft is formed by ectodermal matrix cells and during hair cycling new hair formation is initiated from stem cells in the bulge. In the tooth germ, epithelial folding is regulated by the enamel knot signaling center and it determines the shape of the tooth.

1.5 Wnt/DKK1

During homeostasis, tissue renewal is tightly controlled by the Wnt pathway. However, during pathogenesis it seems that inhibitors of the Wnt pathway, such as DKK1, are upregulated and subsequently affect Wnt mediated repair mechanisms (figure 7) [Schmidt-Ullrich et al.]. Such diseases include multiple myeloma and rheumatoid arthritis, where in both cases it has been demonstrated that secretion of high levels of DKK1 is the cause of the bone lesions. Canonical WNT signals are transduced through Frizzled (FZD) family receptors and LRP5/LRP6 coreceptor to the β -catenin signaling cascade. In the absence of canonical WNT signaling, β -catenin complexed with APC and AXIN is phosphorylated by casein kinase I α (CKI α) and glycogen synthase kinase 3 β (GSK3 β) in the NH₂-terminal degradation box, which is polyubiquitinated by β TRCP1 or β TRCP2 complex for the following proteasome-mediated degradation. In the presence of canonical WNT signaling, Dishevelled (DVL) is phosphorylated by CKI α for high-affinity binding to FRAT. Because canonical WNT signal induces the assembly of FZD-DVL complex and LRP5/6-AXIN-FRAT complex, β -catenin is released from phosphorylation by CKI α and GSK3 β for stabilization and nuclear accumulation. [Yang et al.] Nuclear β -catenin is complexed with T-cell factor/lymphoid enhancer factor (TCF/LEF) family transcription factors and also with Legless family docking proteins (BCL9 and BCL9L) associated with PYGO family coactivators (PYGO1 and PYGO2). The TCF/LEF- β -catenin-Legless-PYGO nuclear complex is the effector of the canonical WNT signaling pathway to activate the transcription of target genes such as *FGF20*, *DKK1*, *WISP1*, *MYC*, and *CCND1*. SFRP1, SFRP2, SFRP3,

SFRP4, SFRP5, WIF1, DKK1, DKK2, DKK3, and DKK4 are secreted-type WNT signaling inhibitors . SFRP family members and WIF1 are WNT antagonists that inhibit WNT binding to FZD family receptors [Zhao et al.]. DKK family members also are WNT antagonists, their interaction with LRP5/LRP6 coreceptor and trigger its endocytosis to prevent formation of the WNT-FZD-LRP5/LRP6 complex for the canonical WNT signaling. Recent studies suggest HF homeostasis is regulated by production autocrine and paracrine factors by dermal papillar cells, one of these factors is DKK-1 (rf). The incubation of dermal papillar cells with dihydrotestosterone determines the induction of DKK1. DKK1 mRNA is up-regulated in 3-6 hours after treatment with 50-100 nM of dihydrotestosterone. ELISA assays showed that DKK-1 is secreted by dermal papillar cells triggering apoptosis of outer root sheath keratinocytes [Kwack et al].

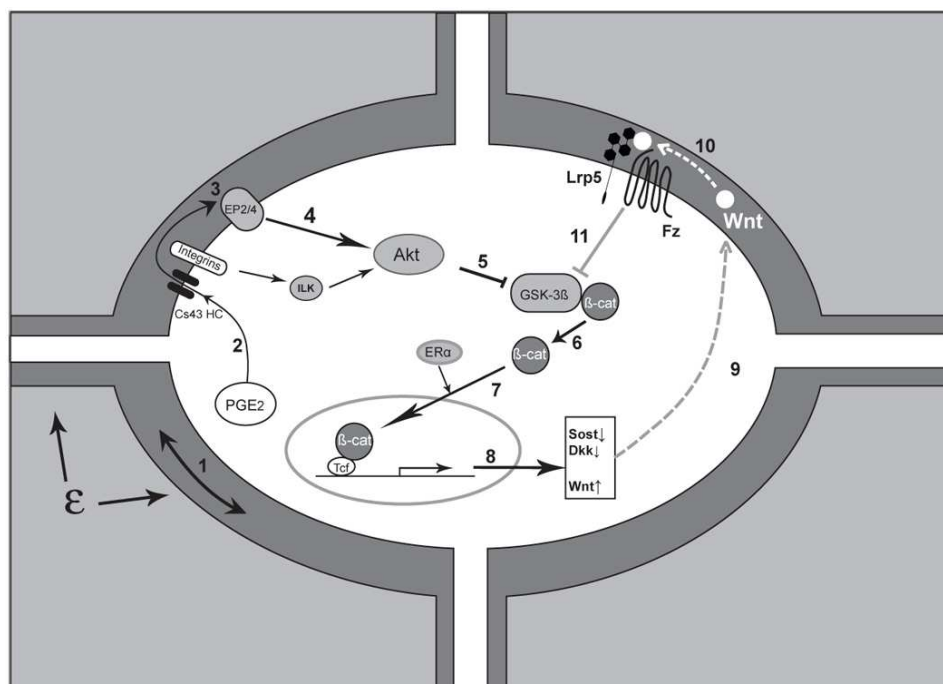


Figure 7. Summary of Wnt/DKK1 relationship. The molecular action of Wnt is described following the numbers. The expression of DKK1 is regulated by the interaction of α -actin with DNA. DKK1 inhibits the Lrp5 interaction with Fz blocking the Wnt pathway (step 9).

1.6 Akt and ERK kinases

Protein kinases regulate diverse cellular functions through the orchestrated propagation and amplification of cellular stimuli into distinct biological responses through coordinated signal transduction cascades. With several hundred kinases encoded in the human genome, almost every signal transduction process is influenced by interconnected phosphorylation events. Deregulation of kinase activity has been implicated in various diseases, ranging from vascular disorders and inflammatory diseases to neurological disorders and cancer. Akt or Protein kinase B (PKB) is a member of the second messenger subfamily of protein kinases [Julien et al.]. The three isoforms of Akt identified have an amino-terminal pleckstrin homology domain, a central kinase domain, and a carboxy-terminal regulatory domain. Akt is the major downstream target of receptor tyrosine kinases that signal via the phosphoinositide (PI) 3-kinase. Receptor-activated PI 3-kinase synthesises the lipid second messenger PI-3,4,5-trisphosphate, leading to the recruitment of Akt to the membrane. Membrane attachment of Akt is mediated by its pleckstrin homology domain binding to PI-3,4,5-trisphosphate or PI-3,4-bisphosphate with high affinity. Activated Akt is implicated in glucose metabolism, transcriptional control, and in the regulation of apoptosis in many different cell types [Pellegrin et al.]. Stimulation of Akt activity protects cells from apoptosis by phosphorylation and inactivation of the pro-apoptotic protein BAD. Conserved signaling pathways that activate the mitogen-activated protein kinases (MAPKs) are involved in relaying extracellular stimulations to intracellular responses [Chen Q et al.]. The extracellular signal-regulated kinase (ERK)

MAPK pathway has been the subject of intense research leading to the development of pharmacologic inhibitors for the treatment of cancer [Gedaly et al.]. ERK is a downstream component of an evolutionarily conserved signalling module that is activated by the Raf serine/threonine kinases [Chen T et al.]. Raf activates the MAPK/ERK kinase (MEK)^{1/2} dual-specificity protein kinases, which then activate ERK^{1/2}. Mitogen-activated protein kinase (MAPK) cascades are key signaling pathways involved in the regulation of normal cell proliferation, survival and differentiation. The ERK/MAPK pathway initially appeared as a linear pipeline that conveyed signals from cell surface receptors to ERK/MAPK, which distributed them to different effectors (figure 8) [Ashton-Beaucage et al.].

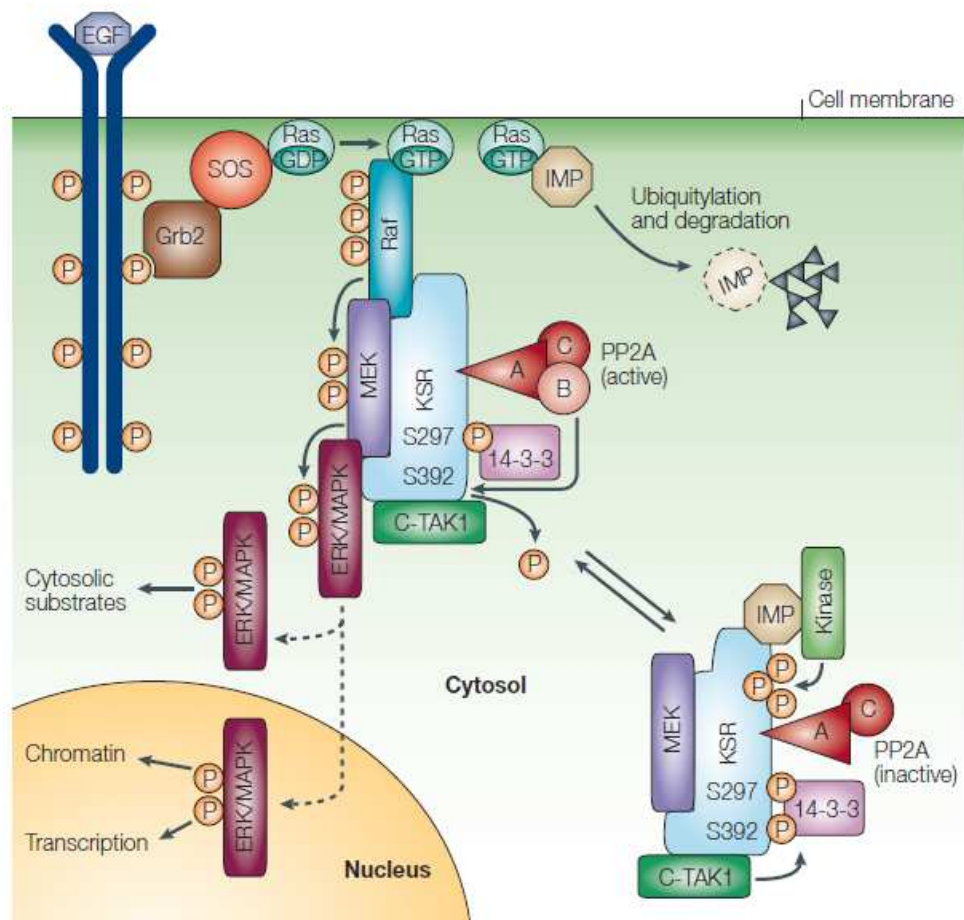
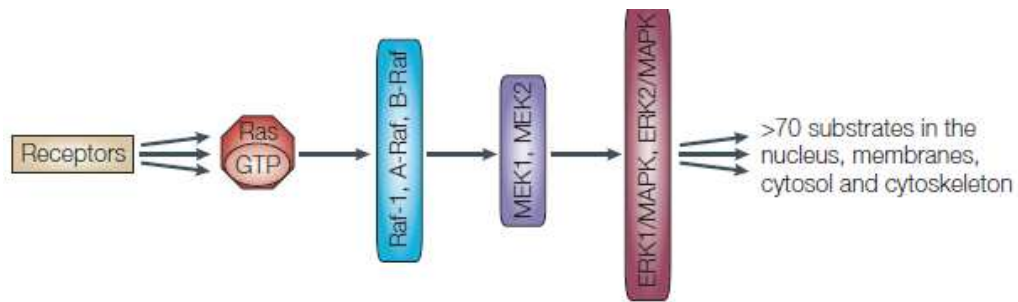


Figure 8. The ERK/MAPK pathway. On stimulation by mitogens such as epidermal growth factor (EGF), activated receptors recruit Ras guanine nucleotide-exchange factors, such as son of sevenless (SOS) through the adaptor protein growth-factor-receptor-bound-2 (Grb2), which generates Ras•GTP. Ras•GTP induces KSR dephosphorylation of S392 by stimulating the binding of the protein phosphatase-2A (PP2A) B subunit to its A and C subunits, which are constitutively associated with KSR. This results in the release of 14-3-3 from this KSR binding site and translocation of KSR to the cell membrane. KSR facilitates the phosphorylation of MAPK and ERK kinase (MEK) by Raf, and enhances the generation of activated extracellular signal-regulated kinase/mitogen-activated protein kinase (ERK/MAPK), which can phosphorylate both nuclear and non-nuclear substrates. [from Walter Kolch Nature Cell Biology 2005]

1.7 Non synthetic molecules

1.7.1 Rutin

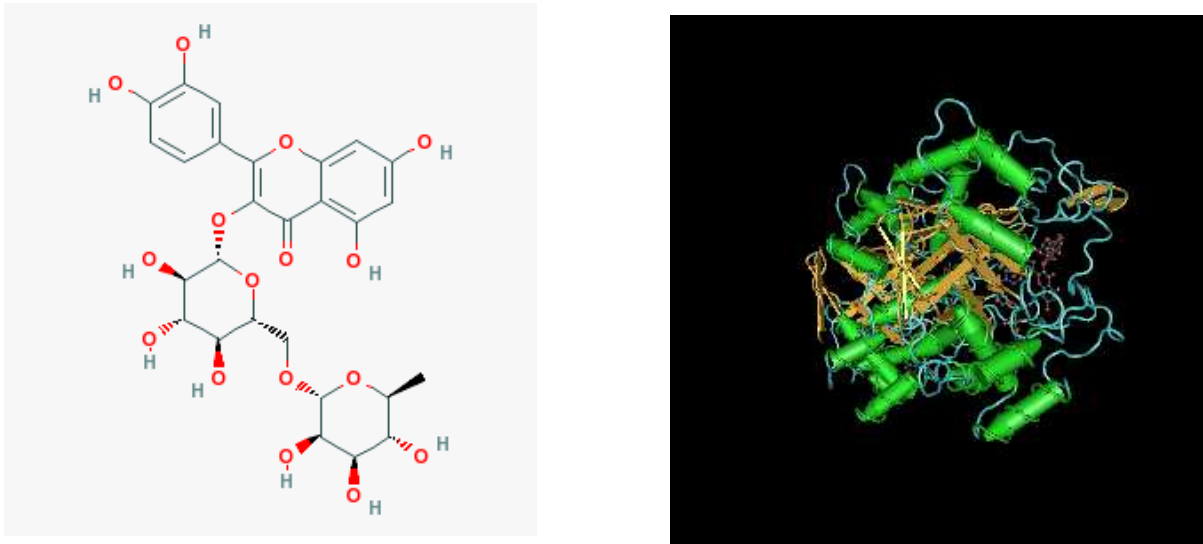


Figure 9. Rutin: chemical and 3D structure

Rutin, also called rutoside, quercetin-3-rutinoside and sophorin, is a citrus flavonoid glycoside found in buckwheat, the leaves and petioles of *Rheum* species, and asparagus. Rutin is also found in the fruit of the Fava D'anta tree (from Brazil), fruits and fruit rinds especially *citrus* fruits (orange, grapefruit, lemon, lime) and berries such as mulberry and cranberries. Its name comes from the name of *Ruta graveolens*, a plant that also contains rutin. It is sometimes referred to Vitamin P, although not strictly a vitamin. Rutin is the glycoside between the flavonol quercetin and the disaccharide rutinose. In Fava d'anta, the synthesis is done via a rutin synthase activity. Rutin can be created by bonding a disaccharide onto the hydroxyl group of Quercetin

(quercetin rutinoside), as well as quercitrin, is a glycoside of the flavonoid Quercetin. [Richetti et al.] As such, the chemical structures of both are very similar, with the difference existing in the Hydroxyl functional group. Both quercetin and rutin are used in many countries as medications for blood vessel protection and are ingredients of numerous multivitamin preparations and herbal remedies [Fonseca et al.]. It can combine with cations, supplying nutrients from the soil to the cells in plants. In humans, it attaches to the iron ion Fe^{2+} , preventing it from binding to hydrogen peroxide, which would otherwise create a highly-reactive free-radical that may damage cells. It is also an antioxidant, and potent VEGF inhibitor (angiogenesis inhibitor), and, therefore, it has been suggested to play a role in inhibiting some cancers. Rutin inhibits platelet aggregation, as well as decreasing capillary permeability, making the blood thinner and improving circulation and it has anti-inflammatory activity [Almeida et al.]. Rutin inhibits aldose reductase activity. Aldose reductase is an enzyme normally present in the eye and elsewhere in the body. It helps change glucose into a sugar alcohol called sorbitol. Rutin also strengthens the capillaries, and, therefore, can reduce the symptoms of haemophilia. It also may help to prevent a common unpleasant-looking venous edema of the legs. Rutin, as ferulic acid, can reduce the cytotoxicity of oxidized LDL cholesterol and lower the risk of heart disease. There is also some evidence that Rutin can be used to treat hemorrhoids, varicosis, and microangiopathy. Hydroxyethylrutosides, synthetic hydroxyethyl acetylations of rutin, are used in the treatment of chronic venous insufficiency [Gong et al.].

1.7.2 Spermidine

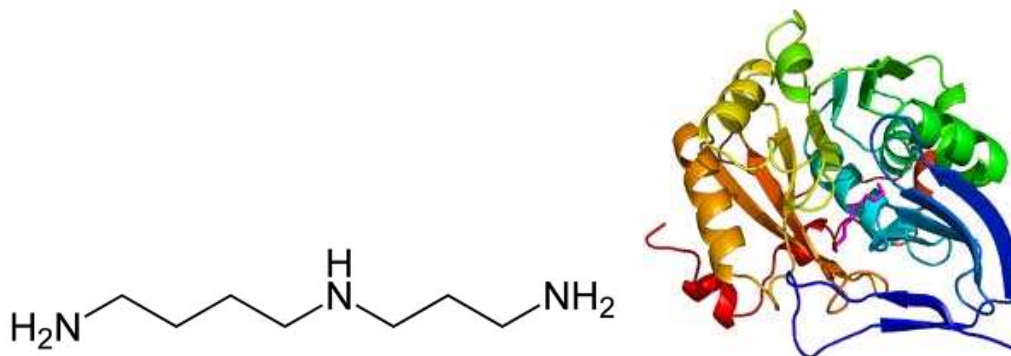


Figure 10. Spermidine: chemical and 3D structure

Spermidine is a polyamine involved in cellular metabolism that can be used to stimulate the enzyme T7 RNA polymerase, a type of RNA polymerase. Spermidine is a ubiquitous polycation that is synthesized from putrescine and serves as a precursor of spermine. Putrescine, spermidine and spermine all are polyamines that participate in multiple known and unknown biological processes. Exogenous supply of spermidine prolongs the life span of several model organisms including (yeast, nematodes, and flies) and significantly reduces age-related oxidative protein damage in mice, indicating that this agent may act as a universal anti-aging drug. Spermidine induces autophagy in cultured yeast and mammalian cells, as well as in nematodes and flies. Genetic inactivation of genes essential for autophagy abolishes the life span-prolonging

effect of spermidine in yeast, nematodes and flies. These findings complement expanding evidence that autophagy mediates cytoprotection against a variety of noxious agents and can confer longevity when induced at the whole-organism level [Garcia-Faroldi et al.].

1.7.3 Zeaxanthin

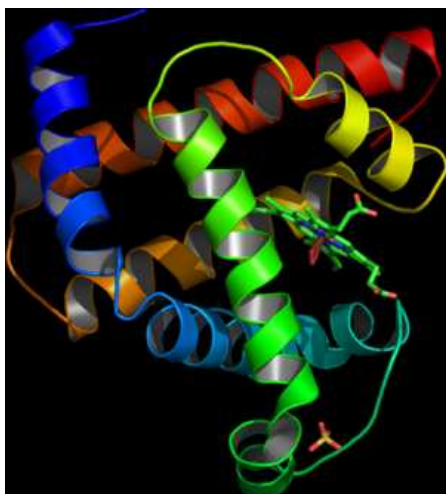
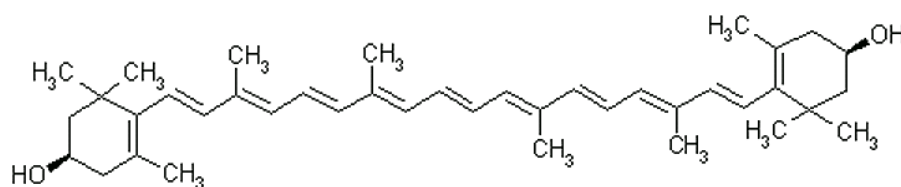


Figure 11. Zeaxanthin: chemical and 3D structure

Zeaxanthin is a bioflavonoid (or flavonoid), which is a type pigment found in almost all herbs, fruits, and vegetables. Bioflavonoids provide the body with anti-inflammatory and antioxidant protection, and are one of the main reasons fruits and vegetables are so healthy to eat. Zeaxanthin belongs to a group of

bioflavonoids known as carotenoids, a group that is further subdivided into two groups: carotenes and xanthophylls. Zeaxanthin is one of the xanthophylls, which are found most abundantly in dark, leafy green vegetables, and are crucial to the good health of the eyes [Ji HF]. The retina of the eye actually contains a lot of zeaxanthin; it helps protect the eye from ultra-violet (UV) damage, and prevents free-radical damage to the retina and the lens of the eye that is associated with diabetic retinopathy, macular degeneration, cataracts, and glaucoma [Bucheli et al.]. The best sources of zeaxanthin are dark-green leafy vegetables, such as greens, kale, and spinach. Zeaxanthin is also found in yellow fruits and vegetables, and egg yolks. Zeaxanthin is a fat-soluble nutrient, which means that it is best absorbed when taken along with foods that contain fat, or in combination with fatty-acid supplements such as fish oil and conjugated linoleic acid (CLA). People that have low-fat diets or diets lacking fruits and vegetables, or with physical conditions that prevent them from properly digesting fat, are at increased risk for carotenoid deficiency [Lecerf et al.].

1.7.4 Epigallocatechin gallate

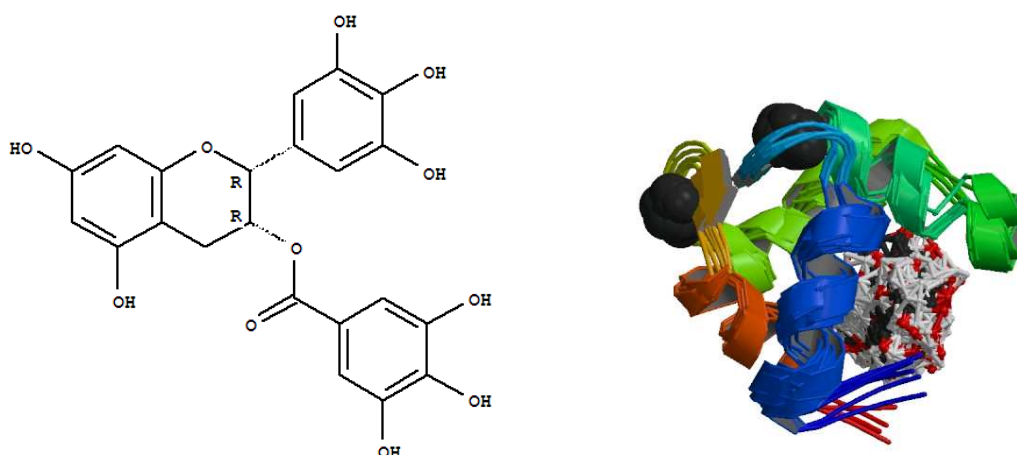


Figure 12. Epigallocatechin gallate: chemical and 3D structure

Epigallocatechin gallate (EGCG), also known as epigallocatechin 3-gallate, is the ester of epigallocatechin and gallic acid, and is a type of catechin. EGCG is the most abundant catechin in most notably tea, among other plants, and is also a potent antioxidant that may have therapeutic properties for many disorders including cancer [El-Mowafy et al.]. It is found in green tea, but not black tea, as EGCG is converted into thearubigins in black teas. In a high temperature environment, an epimerization change is likely to occur, because heating results in the conversion from EGCG to GCG. Thus it is considered inappropriate to infuse green tea or its extracts with overheated water. There has been research investigating the benefit of EGCG from green tea in the treatment of HIV infection, where EGCG has been shown to reduce plaques related to AIDS-related dementia in the laboratory, as well as block gp120 [Monobe et al.]. However, these effects have yet to be confirmed in live human trials, and it does not imply that green tea will cure or block HIV infection, but it

may help regulate viral load as long as it is not involved in adverse drug reactions. The concentrations of EGCG used in the studies could not be reached by drinking green tea. More study into EGCG and HIV is currently underway. There is increasing evidence to show that EGCG, along with other flavonoids, can be beneficial in treating brain, prostate, cervical and bladder cancers. EGCG has been shown to bind and inhibit the anti-apoptotic protein Bcl-xl which has been implicated in both cancer cell and normal cell survival [Rocha et al.].

2. Aim

Androgenetic alopecia has been studied for years; it is very common but unfortunately its causes and therapies are still unknown. With our studying, only with non synthetic molecules, we suggest a way to prevent alopecia and delay its progress.

Three active principles (Spermidine, Rutin and Zeaxanthin) and their mixture were investigated on the regulation of the regression phase of hair cycle. The project was subdivided in two major:

1) in vitro evaluation of anti-apoptotic activity in HFDP cells. We evaluated it in different ways, but especially we measured the activity of caspase-3 in control cells, in apoptotic cells and apoptotic cells and the mixture.

Its activity was investigated in many different ways; we did the special colorimetric assay, where we analyzed the effect of every single molecules on this enzyme. That was the first step of our research, we could evaluate the activity of every single principle, of a couple of molecules and a mixture of three of them. As it is shown in results the best inhibition of caspase-3 activity was made by the mixture of rutin, spermidine and zeaxanthin.

We did also morphological evaluation of the activity of caspase-3 by analyzing HFDP cells morphology and how it changed in apoptosis and how it was preserved by using the mixture.

With western blot analysis we could not only detect caspase 3 but also related enzyme and AKT and Map kinases activity, strictly related with cell life.

2) ability to maintain molecular function in ex vivo human hair bulbs; That was a very interesting assay that allowed us not only to taste the mixtures on cells but also ex vivo on human air bulbs.

3. Materials and Methods

3.1 HFDP cells culture

Human follicle dermal papilla cells (HFDP) are located in the dermal papilla at the base of hair follicles. This primary cells were obtained from Promocell at the passage 2 and were grown in Dermal Papilla Growth Medium in presence of fetal calf serum (FCS; 5% vol/vol) and growth factors (Human recombinant bFGF 100 ng/100ml medium; Bovine pituitary extract 0,4 ml/100 ml medium; Human recombinant insulin 500 microgr/100 ml medium. Cells were maintained at 37°C at 5% CO₂.

3.2 Protein quantification

To perform protein quantification we used the Quick Start™ Bradford protein assay (Biorad), which is a fast, robust and simple one-step method for measuring protein concentrations samples in a variety of solutions. The Bradford method [Anal. Biochem. (1976) 72, 248-254] measures the absorbance shift of the red cationic form of Coomassie Blue G-250 to the blue stable anionic form when bound to arginine and hydrophobic amino acids in proteins. The assay is compatible with a wide range of reagents, such as organic solvents (acetone, acetonitrile, methanol), some detergents (CHAPS, desoxycholate, octylglucoside), most commonly used buffers (PBS, TRIS, HEPES), culture media (Eagles MEM), salt solutions (NaCl₂, MgCl₂, KCl), sugars (sucrose, glucose) and denaturing reagents (DTT, 2-mercaptoethanol,

urea). In this assay Serum Bovine Albumine (BSA) was used as standard. Each sample was quantitated in triple.

3.3 RNA and Protein extraction

Cell protein extracts were obtained by means of TRIzol™ reagent following manufacturer instructions (Invitrogen, Carlsbad, California).

TRIZOL Reagent (U.S.Patent No.5,346,994) is a ready-to-use reagent for the isolation of total RNA from cells and tissues. The reagent, a mono-phasic solution of phenol and guanidine isothiocyanate, is an improvement to the single-step RNA isolation method developed by Chomczynski and Sacchi¹. During sample homogenization or lysis, TRIZOL Reagent maintains the integrity of the RNA, while disrupting cells and dissolving cell components. Addition of chloroform followed by centrifugation, separates the solution into an aqueous phase and an organic phase. RNA remains exclusively in the aqueous phase. After transfer of the aqueous phase, the RNA is recovered by precipitation with isopropyl alcohol. After removal of the aqueous phase, the DNA and proteins in the sample can be recovered by sequential precipitation². Precipitation with ethanol yields DNA from the interphase, and an additional precipitation with isopropyl alcohol yields proteins from the organic phase². Copurification of the DNA may be useful for normalizing RNA yields from sample to sample.

3.3.1 RNA extraction:

- Add 1 mL of TRIzol solution per 10 cm² of culture dish area, and pass the cell lysate through a pipette several times to lyse cells and homogenize the sample.
- Incubate the homogenate for 5 min at room temp. This 5 min room temperature incubation allows nucleoprotein complexes to completely dissociate. Homogenized samples can be stored at -70°C for at least one month.
- Centrifuge at 12,000 xg for 10 min at 4°C and transfer the supernatant to a fresh tube.
- Add 200 µL chloroform per 1 mL of TRI Reagent solution.
- Cap the tubes tightly and shake vigorously for 15 sec.
- Incubate the mixture at room temperature for 10 min.
- Centrifuge at 12,000 x g for 15 min at 4°C, then transfer the aqueous phase to a fresh tube.
- Centrifuge at 12,000 x g for 15 min at 4°C.
- RNA remains exclusively in the aqueous phase whereas DNA and protein are in the interphase and organic phase. The interphase and lower, red, organic phase can be stored
- Add 500 µL of isopropanol per 1 mL of TRIzol solution vortex for 5–10 sec, and incubate at room temp for 5–10 min.
- Vortex at moderate speed for 5–10 sec.
- Incubate the samples at room temp for 5–10 min.
- Centrifuge at 12,000 x g for 8 min and discard the supernatant.
- Centrifuge at 12,000 x g for 8 min.

- Carefully remove the supernatant without disturbing the pellet.
- Precipitated RNA forms a gel-like or white pellet on the side and bottom of the tube.
- Add 1 mL of 75% ethanol per 1 mL of TRIzol solution.
- Add 1 mL of 75% ethanol per 1 mL TRIzol solution used for sample homogenization to each sample to wash the RNA pellets.
- Centrifuge at 7,500 x g for 5 min, remove the ethanol, and briefly air dry the RNA pellet.
- Centrifuge at 7,500 x g for 5 min.
- If the precipitated RNA floats or does not form a compact pellet, repeat the centrifugation at 12,000 x g for 5 min to consolidate the pellet at the bottom of the tube.
- Remove the ethanol wash without disturbing the pellet.
- Remove all residual ethanol by centrifuging again briefly and removing the ethanol that collects with a fine tip pipette.
- Complete removal of ethanol is necessary for the RNA to perform well in downstream applications.
- Air dry the RNA pellet for 3–5 min.
- Do not completely dry the RNA pellet as this will greatly decrease its solubility. Do not dry RNA by vacuum centrifugation.
- Dissolve RNA in the buffer of your choice and store at -70°.

3.3.2 Protein extraction:

Protein are isolated from the phenol-ethanol supernatant obtained after precipitation of DNA with ethanol:

- Add 1,5 mL of isopropanol per 1 mL of TRIzol
- Store samples for 10 minutes at room temperature
- Centrifugate at 12000 xg for 10 minutes
- Remove the supernatant
- Wash the protein pellet 3 times in a solution containing 0,3M guanidine hydrochloride in 95% ethanol. During each wash cycle, store the protein pellet in the wash solution for 20 minutes and centrifugate at 7.500 xg for 5 minutes.
- After the final wash vortex the protein pellet in 2 mL of ethanol.
- Store the protein pellet in ethanol for 20 minutes and centrifugate at 7.500 xg for 5 minutes.
- Vacuum dry the protein pellet for 5-10 minutes.
- Dissolve it in 1% SDS by pipetting.

Sediment any insoluble material by centrifugation at 10.000 xg for 10 minutes and transfer the supernatant to a fresh tube. The sample is ready for use in Western blotting or may be stored at -20° for future use.

3.4 SDS Page, Western blotting and protein detection

3.4.1 Protein sample preparation for electrophoresis

50-75 µg of protein samples (cell lysate or tissue homogenized), previously TCA precipitated (paragraph 2.) or not, are combined with Novex Tris-Glycine SDS sample buffer 2X (Invitrogen) containing 5% 2-β mercaptoethanol (70mM) in a microcentrifuge tube. In the case of TCA precipitation, Tris buffer is sometimes added to adjust pH if TCA residues are still present in sample resuspension. Many proteins have significant hydrophobic properties and may be tightly associated with other molecules, such as lipids, through hydrophobic interaction. Heating the samples to at least 60°C shakes up the molecules, allowing SDS to bind in the hydrophobic regions and complete the denaturation. Thus, the samples are boiled for 5-10 min to fully denature the proteins and left at room temperature until ready to load onto the gel. Molecular weight marker (5µL) (Bio-Rad) is aliquoted in a separate tube and boiled for 1 min.

3.4.2 SDS Page

Sodium dodecyl sulfate-polyacrylamide gel electrophoresis (SDS-PAGE) is probably the most common analytical technique used to separate and characterize proteins, using a discontinuous polyacrylamide gel as support medium and SDS to denature the proteins. SDS (also called lauryl sulfate) is an anionic detergent bound by a polypeptide chain in proportion to its relative molecular mass. The negative charges on SDS destroy most of the complex structure of proteins, and are strongly attracted toward an anode in an electric

field. Polyacrylamide gels restrain larger molecules from migrating as fast as smaller molecules. Because the charge-to-mass ratio is nearly the same among SDS-denatured polypeptides, the final separation of proteins is dependent almost entirely on the differences in relative molecular mass of polypeptides. In a gel of uniform density the relative migration distance of a protein (R_f) is negatively proportional to the log of its mass. If proteins of known mass are run simultaneously with the unknowns, the relationship between R_f and mass can be plotted, and the masses of unknown proteins estimated. Protein separation by SDS-PAGE can be used to estimate relative molecular mass, to determine the relative abundance of major proteins in a sample, and to determine the distribution of proteins among fractions. Acrylamide is the material of choice for preparing electrophoretic gels to separate proteins by size. Acrylamide mixed with bisacrylamide forms a cross-linked polymer network when the polymerizing agent, ammonium persulfate, is added. The ammonium persulfate produces free radicals faster in the presence of TEMED (N,N,N,N'-tetramethylethylenediamine). The size of the pores in a gel is inversely related to the amount of acrylamide used. Very large polypeptides cannot penetrate far into a gel and thus their corresponding bands may be too compressed for resolution. Polypeptides below a particular size are not restricted at all by the gel, and regardless of mass they all move at the same pace along with the tracking dye. Gel concentration (%T) should be selected to resolve precisely proteins of interest. A typical gel of 7% acrylamide composition separates polypeptides with molecular mass between 45 and 200 kDa. There are two types of buffer systems used in PAGE electrophoresis: continuous and discontinuous systems. A continuous system has only a single

separating gel and uses the same buffer in the tanks and the gel. In a discontinuous system, a non-restrictive large pore gel, called stacking gel, is layered on top of a separating gel called resolving gel. Each gel is made with a different buffer, and the tank buffers are different from the gel buffers. The stacking gel has a lower concentration of acrylamide (larger pore size), lower pH and a different ionic content. This allows the proteins to be concentrated into a tight band before entering in the resolving gel. The resolving gel may consist of a constant acrylamide concentration or a gradient of acrylamide concentration (high percentage of acrylamide at the bottom of the gel and low percentage at the top). A gradient gel is prepared by mixing two different concentrations of acrylamide solution to form a gradient with decreasing concentrations of acrylamide. As the gradient forms, it is layered into a gel cassette. This latter gel is recommended for separation of a mixture of proteins with a greater molecular weight range.

In our experimental conditions, continuous gel was running under reducing and denaturant conditions. Gel preparation procedures and running conditions used are described in the following protocol:

- Assemble glass plate sandwich using two clean glass plates and two 75-mm spacers. Assemble the casting frame and stand as described by manufacturer.
- In a clean falcon, prepare the resolving gel solution, mixing the ingredients as described in Table 11, remembering that AP and TEMED must be added at the end. Be careful not to generate bubbles.

- Pour the resolving gel to a level about 1 cm from the top. Wait 1 min, then layer the top of the gel with saturated butyl alcohol (this will help the gel to solidify quickly in the absence of air).
- Wait another 15-20 min for the gel to polymerize. Pour off the top layer of butyl alcohol and rinse with distilled water. Dry off as much of the water as possible, using absorbent paper.
- In a clean falcon, prepare the stacking gel as described in Table 11, being careful not to generate bubbles.
- Pour the resolving gel till the space is full, then put in the appropriate comb. (The difference in the pH of the two layers is what causes the stacking of the proteins. Thus, if the proteins are not stacking properly check the pH of the buffers).
- Allow the top portion to solidify and then carefully remove the comb or store at 4°C in humidified condition, until use.
- Place gel in opposite side of apparatus (Mini-PROTEAN 3-Cell, Bio-Rad).
- Slowly add 1x Running buffer.
- Load samples and molecular weight marker.
- Run the gel at 60V until the blue dye overpass stacking phase, and then run it at 110 V until the blue dye reaches the bottom or runs off. At this time, the run is stopped, cables removed. The gel is removed from the cassette and can be processed for western blotting.

Table 1. Resolving and Stacking gel solution recipes.

Reagents	Running gel (1x)				Stacking gel (1x)
	7%	10%	12%	15%	3%
Acrylamide percentage					
dH ₂ O (ml)	7.2	15.3	12.3	10.2	3.075l
30%/0.8% Acrylamide/Bis (ml)	7.5	7.5	7.5	7.5	1.25
4x Lower Tris Buffer (ml)	0.15	0.15	0.15	0.15	0.025
10% SDS (ml)	15.0	6.9	9.9	12.0	0.67
APS (ml)	0.15	0.15	0.15l	0.15	0.025
TEMED (ml)	0.02	0.02l	0.02	0.02	0.005

3.4.3 Western blotting and protein detection

The term “blotting” refers to the transfer of biological samples from a gel to a membrane and their subsequent detection on the surface of the membrane. Western blotting was introduced by Towbin and colleagues [1989] and is now a routine technique for protein analysis. The specificity of the antibody-antigen interaction enables a single protein to be identified in the midst of a complex protein mixture. Western blotting is commonly used to identify a specific protein in a complex mixture and to obtain qualitative and semiquantitative data about that. The first step in a western blotting procedure is to separate the macromolecules using gel electrophoresis. Following electrophoresis, the separated molecules are transferred onto a second matrix, generally a

nitrocellulose or polyvinylidene fluoride (PVDF) membrane. Next, the membrane is blocked to prevent any nonspecific binding of antibodies to the surface of the membrane. The transferred protein is complexed with an enzyme-labeled antibody as a probe. An appropriate substrate is then added to the enzyme and together they produce a detectable product such as a chromogenic or fluorogenic precipitate on the membrane for colorimetric or fluorimetric detection, respectively. The most sensitive detection methods use a chemiluminescent substrate that, when combined with the enzyme, produces light. This output can be captured using film, a CCD camera or a phosphorimager designed for chemiluminescent detection. Whatever substrate is used, the intensity of the signal correlates with the abundance of the antigen on the blotting membrane. In our experimental procedure, western blotting and protein detection protocols are the following:

- Cut a piece of nitrocellulose membrane (Hybond-ECL, Amersham Biosciences). Wet the membrane in dH₂O. Soak membrane in 1x Transfer buffer for 10 min.
- Pre-wet the sponges, filter papers (slightly bigger than gel) in 1x Transfer buffer. Assemble sandwich (sponge-paper-gel-membrane-paper-sponge) for the electroblotting apparatus (Mini Trans-Blot Electrophoretic Transfer Cell, Bio-Rad).
- Transfer for 1 hr at 100 V with a cold pack and prechilled buffer.
- After transfer is complete, turn off power supply and remove cathode plate of blotter. Remove transfer membrane and cut lower right corner of membrane to mark orientation of gel.

- Staining the membrane with Ponceau's dye and the gel with Coomassie Blue dye to verify the correct transfer.
- Remove Ponceau's staining, washing the membrane with dH₂O.
- Block the nitrocellulose membrane in TBS with 0,05% Tween-20 (v/v) (T-TBS), containing 5% skim milk (w/v) for at least 60 min on a rocking platform.
- Wash the nitrocellulose membrane 3 times in T-TBS for 10 min each on a rocking platform.
- Incubate the nitrocellulose membrane on a rocking platform with primary antibody diluted in T-TBS, overnight at 4°C.
- Wash the nitrocellulose membrane 3 times in T-TBS for 10 min each on a rocking platform.
- Incubate with secondary antibody horseradish peroxidase-conjugate diluted in 5% milk T-TBS for 60-90 min on a rocking platform at room temperature.
- Wash the nitrocellulose membrane 3 times in T-TBS for 10 min each on a rocking platform.
- Wash the nitrocellulose membrane once in TBS to remove the excess of tween.
- Detect proteins by means of an enhanced chemiluminescence detection system (ECLTM, Amersham).
- After incubation of 5 min with ECL, blots are placed in a sheet protector and exposed to Kodak X-Omat Blue Film (Blue X-ray Film) (Perkin Elmer) for different times. Several exposures allow better densitometric analysis.

- Autoradiography films are automated processed with an Automated x-ray film developer (Kodak M35A X-OMAT processor).

Primary antibodies used in experimental procedures:

- anti- β -actin, clone K3004 (dilution 1:1000 in T-TBS 0.05%) (Santa Cruz Biotechnology).
- anti-Akt, (dilution 1:1000 in T-TBS 0.05%) (Cell Signaling).
- anti-phospho Akt, (dilution 1:1000 in T-TBS 0.05%) (Cell Signaling).
- anti-Erk, (dilution 1:1000 in T-TBS 0.05%) (Cell Signaling).
- anti-phospho Erk, (dilution 1:1000 in T-TBS 0.05%) (Cell Signaling).
- PARP, (dilution 1:200 in T-TBS 0.05%) (Santa Cruz Biotechnology).
- Caspase-3, (dilution 1:200 in T-TBS 0.05%) (Santa Cruz Biotechnology).
- EDA receptor, (dilution 1:1000 in T-TBS 0.05%) (R&D).

Secondary antibodies used in experimental procedures:

- anti rabbit IgG-HRP (dilution 1:10.000 in T-TBS 0.05%) (Chemicon International).
- anti goat IgG-HRP (dilution 1:10.000 in T-TBS 0.05%) (Chemicon International).
- Anti mouse IgG-HRP (dilution 1:5.000 in T-TBS 0.05%) (Chemicon International).

Nitrocellulose membrane stripping

After visualizing protein of interest, it is possible to strip off the first set of protein probes so that different proteins on the blot may be detected using a second set of specific probes. When possible, this technique saves the time

and resources that would be necessary to electrophorese another sample and transfer it to new sheet of membrane. Stripping generally involves soaking the blot in a buffer that is sufficiently harsh to dissociate the affinity interactions between antibodies and the target sample protein that was transferred to the membrane. The goal is to find a stripping condition that is efficient in removing the probes without also removing or damaging the target proteins on the blot. Because every antibody-antigen affinity interaction and target protein is unique, no one stripping condition is appropriate for all situations. Empirical testing and some optimization are necessary to determine appropriate stripping conditions for a particular western blot system. In most cases, conditions can be optimized to make at least one round of stripping and reprobing possible. In some cases, several rounds of stripping and reprobing are possible.

In our experimental condition, the stripping protocol consists in:

- Wash abundantly the nitrocellulose membrane with T-TBS on a rocking platform.
- Incubate the membrane with Stripping Buffer at 50°C for 30 min. Adding 0.5 M NaCl to the stripping buffer slightly reduces the background from multiple probings.
- Wash abundantly the nitrocellulose membrane with TBS on a rocking platform.
- Return to membrane blocking and primary antibody incubation as previously described.

Densitometric analysis

Exposures of the same membrane for different times were acquired using GelDoc™ image capture system (Bio-Rad), following Manufacturer's

instructions. The autoradiograms were quantified using Quantity One™ and Image J software. The data were then analyzed with suitable statistic methods.

Polyacrylamide gel staining

After western blotting procedure, gel staining allows to verify the correct loading of protein samples and the correct protein transfer to nitrocellulose membrane. A commonly used stain for detecting proteins in polyacrylamide gels is 0.1% Coomassie Blue dye in 50% methanol, 10% glacial acetic acid. Acidified methanol precipitates the proteins. Staining is usually performed overnight on a rocking platform. The dye penetrates the entire gel, and sticks permanently to the proteins. Excess dye is washed out by destaining procedure with acetic acid/methanol washes on a rocking platform. Destaining in two steps (first using 50% methanol, 10% acetic acid for 1-2 hours, and then using 7% methanol, 10% acetic methanol) provided a better efficiency. Finally, gels can be dried or photographed for later analysis.

3.5 Caspase-3 activity

The proteolytic activity of caspase-3 was evaluated by means of a colorimetric assay ApoTarget™Caspase-3/ CPP32 with DEVD-pNA as a substrate (BioSource International, Camarillo, CA). The colorimetric substrate (Ac-DEVD-pNA) provided in the Assay System, Colorimetric, is labeled with the chromophore *p*-nitroaniline (pNA). pNA is released from the substrate upon

cleavage by DEVDase. Free pNA produces a yellow color that is monitored by a spectrophotometer at 405 nm. The amount of yellow color produced upon cleavage is proportional to the amount of DEVDase activity present in the sample. The assay was performed following the instructions of the provider. Briefly, for each sample was used the same amount of protein extract (200 μ g) and each sample was assayed in double. The measure of absorbance at 405 nm was performed by means of an automatic spectrophotometer (MPT Reader DV990 BVG).

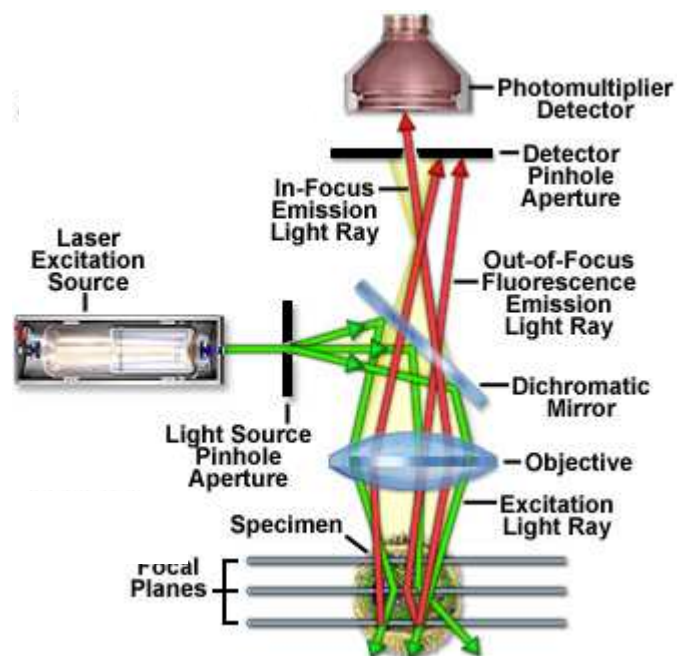
3.6 Confocal microscopy

Confocal microscopy offers several advantages over conventional optical microscopy, including

controllable depth of field, the elimination of image degrading out-of-focus information, and the ability to collect serial optical sections from thick specimens.

The key to the confocal approach is the use of spatial filtering to eliminate out-of-focus light or flare in specimens that

are thicker than the plane of focus. In recent years, there has been a tremendous explosion in the popularity of confocal microscopy, due in part to the relative ease with which extremely high-quality images can be obtained



from specimens prepared for conventional optical microscopy. In a conventional widefield microscope, the entire specimen is bathed in light from a mercury or xenon source, and the image can be viewed directly by eye or projected onto an image capture device or photographic film. In contrast, the

method of image formation in a confocal microscope is fundamentally different. Illumination is achieved by scanning one or more focused beams of light, usually from a laser or arc-discharge source, across the specimen. This point of illumination is brought to focus in the specimen by the objective lens, and laterally

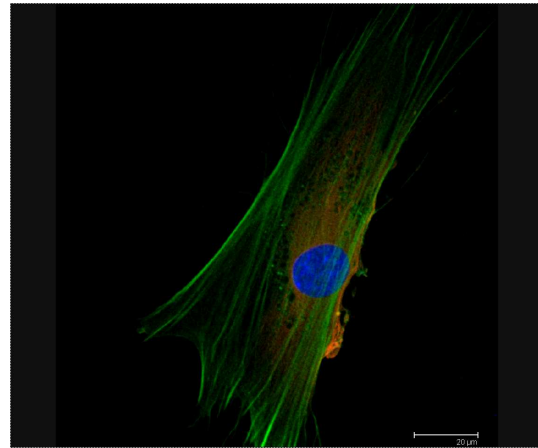


Figure 14. Confocal microscopy image of Caspase-3 and Phalloidin immunostaining. Caspase3(RED) and Phalloidin (GREEN) staining was performed in HFDP cells, previously fixed on slide with paraformaldehyde procedure. In blue, nuclei staining with DAPI dye. Immunofluorescence image assessed

scanned using some form of scanning device under computer control. The sequences of points of light from the specimen are detected by a photomultiplier tube (PMT) through a pinhole (or in some cases, a slit), and the output from the PMT is built into an image and displayed by the computer (Figure 13). Although unstained specimens can be viewed using light reflected back from the specimen, they usually are labelled with one or more fluorescent probes.

Specimen Preparation and Imaging

The procedures for preparing and imaging specimens in the confocal microscope are largely derived from those that have been developed over many years for use with the conventional wide field microscope. In the

biomedical sciences, a major application of confocal microscopy involves imaging either fixed (Figure 14) or living cells and tissues. Cells have usually been labeled with one or more fluorescent probes. A large number of fluorescent probes are available that, when incorporated in relatively simple protocols, specifically stain certain cellular organelles and structures. Among the plethora of available probes are dyes that label nuclei, the Golgi apparatus, the endoplasmic reticulum, and mitochondria, and also dyes such as fluorescently labelled phalloidins that target polymerized actin in cells. Regardless of the specimen preparation protocol employed, a primary benefit of the way in which confocal microscopy is carried out is the flexibility in image display and analysis that results from the simultaneous collection of multiple images, in digital form, into a computer.

Critical aspects of Confocal microscopy

Quantitative three-dimensional imaging in fluorescence microscopy is often complicated by artifacts due to specimen preparation (e.g. autofluorescence problems, retractile structures presence, presence or absence of highly stained structures, immersion oil, coverslip thickness etc.), controllable and uncontrollable experimental variables, or configuration problems with the microscope (e.g. optical component alignment, objective magnification, bleaching artifacts, aberrations, quantum efficiency, and the specimen embedding medium).

In our experimental conditions, the immunofluorescence experiments were assessed by confocal microscopy TSC SP2 Leica.

3.6.1 Cell culture immunofluorescence

Cell staining for confocal microscopy analysis was performed according to following procedures:

Preparation of cover glasses:

- Wash cover glasses for 30 min in running tap water.
- Rinse with dH₂O.
- Incubate cover glasses in 40 µg/ml poly-L-lysine (MW ~70-90kDa) overnight at 37°.
- Wash cover glasses for 1 hour in running tap water.
- Rinse cover glasses 3 times for 5 min each in dH₂O.
- Dry cover glasses on filter paper in a dust-free area.
- Sterilize cover glasses inside the laminar flow chamber under UV light for at least 4 hours.

Cell culture

- Detach cell from the plastic surface by incubating them in trypsin solution.
- Resuspend detached cells in culture medium and transfer them to culture dishes with the cover glasses.
- Culture cells up to semi-confluency.

Paraphormaldeid fixation

The paraformaldehyd fixation is an easy and rapid fixation method. It works by precipitating cellular proteins onto the coverslip. There is no need to permeabilise the cells and there is no quenching of the fixative required.

However, this method has provided low structural cell preservation since lipids and soluble proteins are extracted from the cell.

After cell fixation, the protocol used is the following:

- Wash cells with PBS. Drain off culture medium and rinse cover slips with PBS. Drain off PBS with any of the above mentioned fixation methods.
- Wash in PBS 3-times 5 min.
- Permeabilize with 0.01% Triton X-100 in PBS for 30 sec (if needed).
- Wash in PBS 3-times 5 min
- Incubate in 1% BSA, PBS pH 7.5 for 30 min to block unspecific binding of the antibodies. (alternative blocking solutions are: 1 % gelatine, 1 % bovine or horse serum).
- Incubate with primary antibody in 1% BSA, PBS pH 7.5 for 60 min (or over night at room temperature, depending on antibody concentration and the accessibility of the antigen).
- Wash with PBS pH 7.5, 3-times 10 min.
- Incubate 2nd antibody in 1% BSA, PBS pH 7.5, 60 min at room temperature.
- Wash with PBS pH 7.5, 3-times 10 min.
- Incubate in 0.1-1 mg/ml Hoechst or DAPI (DNA stain) for 10 min.
- Rinse with PBS.
- Mount in PPD-mounting medium.
- Seal with nail polish.

Primary antibodies used:

- Phalloidin, (dilution 1:100 in PBS) (Molecular Probes).
- Keratin 8-18, (dilution 1:100 in PBS) (Lab Vision).

- Caspase-3, (dilution 1:100 in PBS) (Santa Cruz Biotechnology).
- EDA receptor, (dilution 1:100 in PBS) (R&D).
- EDA1 (dilution 1:100 in PBS) (R&D).

Secondary antibodies:

- anti rabbit IgG (dilution 1:1000 in PBS) (Invitrogen).
- anti goat IgG (dilution 1:1000 in PBS) (Invitrogen).
- Anti mouse IgG (dilution 1:1000 in PBS) (Invitrogen).

3.7 TUNEL assay

The DeadEnd™ Fluorometric TUNEL System(a) is designed for the specific detection and quantitation of apoptotic cells within a cell population. The system is non-radioactive and provides for simple, accurate and rapid detection of apoptotic cells in situ at the single-cell level or in cell suspensions. The system can be used to assay apoptotic cell death in many systems, including cultured cells and formalin-fixed, paraffin-embedded tissue sections. The DeadEnd™ Fluorometric TUNEL System measures nuclear DNA fragmentation, an important biochemical hallmark of apoptosis in many cell types.

3.7.1 Apoptosis Detection

- Fix: Immerse slides in 4% formaldehyde in PBS for 25 minutes at 4°C.
- Wash: Immerse slides twice in PBS, 5 minutes each time.

- Permeabilize: Immerse slides in 0.2% Triton® X-100 in PBS for 5 minutes.
- Wash: Immerse slides twice in PBS, 5 minutes each time.
- Equilibrate: Add 100µl Equilibration Buffer. Equilibrate at room temperature for 5–10 minutes.
- Label: Add 50µl of TdT reaction mix to the cells on an area no larger than 5 square centimeters. Do not allow cells to dry completely. Cover slides with Plastic Coverslips to ensure even distribution of the mix. Incubate slides for 60 minutes at 37°C in a humidified chamber; avoid exposure to light from this step forward.
- Stop Reaction: Remove Plastic Coverslips. Immerse slides in 2X SSC for 15 minutes.
- Wash: Immerse slides three times in PBS, 5 minutes each time.
- Mount: Add mounting medium to slides.
- Counterstain: To visualize all nuclei, use Vectashield® with DAPI.
- Analyze: Detect localized green fluorescence of apoptotic cells by fluorescence microscopy. DAPI-stained nuclei will be blue.

3.8 Prevention of protein degradation in ex-vivo hair bulbs

Since drug treatment had a very favourable effects against apoptotic phenomena, it was relevant to test whether such treatment was also be affective in preventing the hair bulb decay following its extraction and *in vitro* incubation for 24 hours. In the first assay, 50 human hair bulbs were extracted by means of a fine forceps from a healthy donor. After the isolation the same

number of follicles were batched in PBS with proteases inhibitors (PMSF 1mM; NaVO₄ 10mM and NaF 1 mM) in presence or absence of compound mixture A (SP 0.5 mg/cps; RU 2.5 mg/cps; ZEA 2 mg/cps) incubated for different times (0 min; 30 min and 24 hours) at 37°C in presence of 5% CO₂. At the end of the incubation period, bulbs were centrifuged at 10.000xg for 1 minute at room temperature. Supernatant was removed and the bulbs were re-suspended in 1 ml of trizol™ and processed for protein extraction (see materials and methods). Proteins were loaded on SDS gel electrophoresis under reducing and denaturing conditions. The activity of AKT and Erk was investigated by means of specific antibodies against phosphorylated forms of the protein

A second ex-vivo assay was performed on hair bulbs from 3 healthy female subjects. 152 bulbs, after removal of the hair, were mixed and separated in 8 vials for 8 different treatment conditions (19 bulbs for each treatment) following scheme outlined below.

- Time of incubation =0'

Sample 1 - F - Igf-1

“ 2 - F +Igf-1

“ 3 +F - Igf-1

“ 4 +F +Igf-1

- Time of incubation =24h

Sample 5 - F - Igf-1

“ 6 - F +Igf-1

“ 7 +F - Igf-1

“ 8 +F +Igf-1

- Mixture of compounds used: A (SP 0.5 mg/cps; RU 2.5 mg/cps; ZEA 2 mg/cps)
- Insulin growth factor-1 (IGF-1): 50ng/ml

Insulin-like growth factor-I (IGF-1) and high-affinity IGF-binding proteins (IGFBPs) are expressed in the hair follicle, suggesting a role of the IGF signalling pathway in follicle biology. In the skin, IGF-I has been reported to be exclusively expressed by mesenchymal cells of the dermis and the dermal papilla. Its receptor, IGF-1R, is synthesized in mesenchymal as well as in epithelial cells. Gene expression has been demonstrated for the dermal papilla and cells of the hair matrix. IGF-1, its receptor and several IGFBPs are expressed in various compartments of the human and murine hair follicle. In humans, IGF-binding protein 3 is mainly expressed in the dermal papilla of hair producing follicles. Further reports reveal the capability of keratinocytes to produce insulin-like growth factor binding protein 3 (Igfbp3). Furthermore, IGF-I appeared to be essential to maintain in vitro cultured human hair follicles in the active, hair producing state. IGF-I-mediated effects on differentiation processes in the hair follicle have not yet been reported. For this reason we investigated the effect of IGF-I (50 ng/ml) in our experimental conditions.

Samples from 1 to 4 were immediately precipitated by centrifugation (see above), dissolved in 1 ml of trizol™ and processed for protein extraction. Samples from 5 to 8 were incubated at 37°C in presence of 5% CO₂ for 24 hours and at the end of incubation period they were processed as reported previously. Proteins concentration was determined by using the Bredford's

method with BSA as a standard. The same amount of protein (50 μ g) was loaded on SDS acrylamide GEL and electroblotted on nitrocellulose membrane.

We investigated the expression of following proteins:

- AKT
- PHOSPHO AKT
- ERK
- PHOSPHO ERK
- PARP
- EDAR

3.9 Statistical Analysis

Western blotting results were statistically evaluated using Fisher's exact test and the *t* test; the immunohistochemical data were analysed using the χ^2 test. All of the analyses were performed using Ministat 2000 (2.1 version, Pubblicazioni Medico Scientifiche, Udine, Italy) and GraphPad Prism 4.0 software; p values of <0.05 were considered statistically significant.

3.10 Materials

Running buffer 1X

192 mM Glycin (BDH; Manchester- UK)

0.1% SDS (Sigma)

25 mM Tris (Biorad)

Sample buffer 2X

0.5 M Tris-HCl (BDH) pH 6.8

20% Glycerol (Sigma)

10% SDS (Sigma)

0.1% Bromophenol blue (Biorad)

0.5% β -mercaptoetanol (Sigma).

Transfer buffer 1X

19 mM Glycin (BDH)

2.5 mM Tris Base (Biorad)

2% Methanol (BDH)

Ponceaus red

0.2% (w/v) Ponceau's (Sigma)

3% (w/v) TCA (Sigma)

3% sulfosalicylic acid (Sigma)

TBS

20 mM Tris (Biorad)

500 mM NaCl (BDH)

T-TBS 0.05% or 0.1%

20 mM Tris (Biorad)

500 mM NaCl (BDH)

0.05% or 0.1% Tween20 (BDH)

Blocking buffer

5% not fat milk powder (Merck; Francoforte - DH) in T-TBS 0.05%.

Stripping solution

2% SDS (Sigma)

62.5 mM Tris-HCl pH 6.7 (BDH)

100 mM β -mercaptoetanol (Sigma)

Homogenization buffer

25mM Tris-Hcl pH 7.4 (Biorad)

1mM EGTA (BDH)

250 mM Saccarose (BDH)

1% NP40 (Sigma)

1% Triton X-100 (BDH)

0.4 mM EDTA (BDH)

plus protease inhibitors:

50 mM NaF (Sigma)

1 mM NaVO₃ (Sigma)

4 mM PMSF (Sigma)
1 M Benzamidine (Sigma)
1 M NaN₃ (Sigma)
10 µg/ml Aprotinin (Sigma)
10 µg/ml Leupeptin (Sigma)
Lowry-Ciocalteau's protein assay
BSA (Sigma)
Na₂CO₃ al 2% (Merk)
CuSO₄ 0.5% (BDH)
NaK tartrato 1% (BDH)
Folin Ciocalteau's (Fluka; Buchs - SW)
PBS 0.01 M
137 mM NaCl (BDH)
2.7 mM KCl (BDH)
1.47 mM KH₂PO₄ (BDH)
8.1 mM Na₂HPO₄ (BDH)
in dH₂O.

Immunocytochemistry reagents

Xilene (BDH)
Ethanol 100% (BDH)
sodium citrate 0.01M (pH=6) (Sigma)
NH₄Cl 0.05 M (BDH)
H₂O₂ 1% (Merck)
BSA 1.5% (Sigma)
Triton 0.2% (BDH)
DAB 3% (Sigma)
A549 complete medium
87% RPMI1640 (Euro Clone; St. Louis - MO)
10% FBS(Euro Clone)
1% Penicillin G potassic salt (100 U/ml) (Euro Clone)
1% Streptomycin Sul fate (100 µg/ml) (Euro Clone)
1% Glutamine (Euro Clone).

Lysis buffer

2% SDS (Sigma)

0.1 M CH₃COONa (Sigma)

5 mM EDTA (BDH)

in dH₂O.

TBE 1X

0.009 M Tris Borate (Sigma)

0.002 M EDTA (BDH)

in H₂O_{mQ}.

Loading dye

0.025% bromophenol blue (Sigma)

0.25% xylene cyanol (Sigma)

30% Glycerol (BDH)

4. Results

4.1 Anti-apoptotic effect of compounds under investigation

Apoptosis in HFDP cells was induced by exposure to staurosporin added to the normal growth medium at the final concentration of 1 μ M. In figure 14 it is shown that staurosporin enhanced by about four fold the activity of caspase-3 within 24 hours. A shorter incubation (6 hours) was ineffective and caspase-3 activity did not increase. The experiment was run in duplicate.

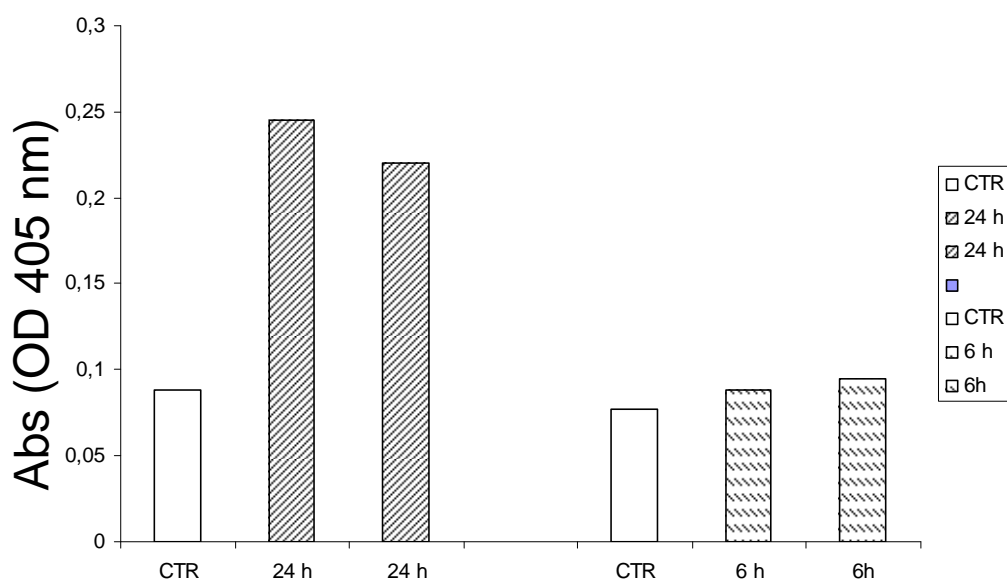


Figure 15. Induction of caspase-3 activity in presence of 1 μ M Staurosporin at 24 (▨) and 6 (▩) hours.

Thus the 24 hour incubation period was chosen as the experimental time frame. The action of investigated compounds was evaluated by adding them at the proper concentration to the growth medium immediately after 1 μ M staurosporin. Following the standard incubation period of 24 hours, cells were washed once with cold PBS (4 $^{\circ}$ C), then proteins were extracted in lysis buffer

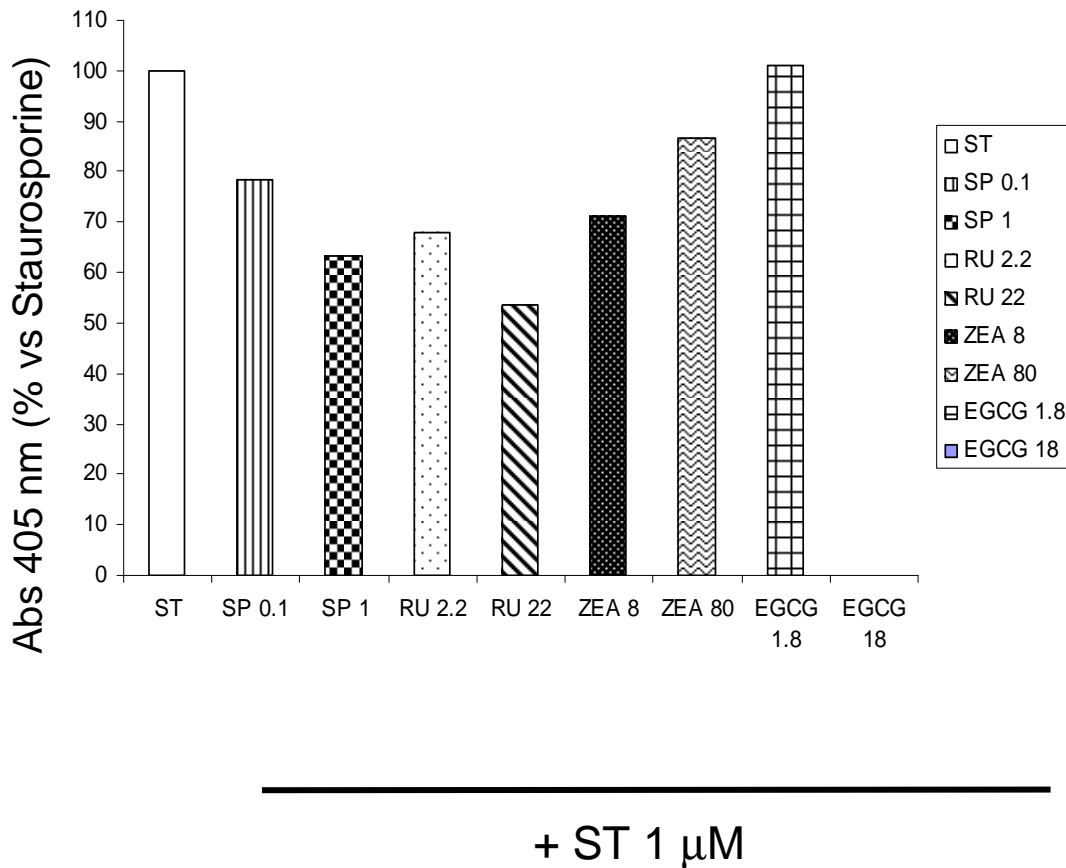
(provided by the supplier of caspase-3 assay kit). Proteins concentration was determined by Quick Start™ Bradford method with BSA as a standard. The activity of caspase-3 was determined using 200 µg of total proteins.

Table 2. Concentrations of active principles applied used in the test of caspase-3 activity

	[µM]	[µg/ml]
SPERMIDINE (SP)	0.1	0.026
SPERMIDINE (SP)	1	0.264
RUTIN (RU)	2.2	1.34
RUTIN (RU)	22	13.42
ZEAXANTHINE (ZEA)	8	4.54
ZEAXANTHINE (ZEA)	80	45.44
EPIGALLOCATECHIN GALLATE (ECG)	1.8	0.824
EPIGALLOCATECHIN GALLATE (ECG)	18	8,24

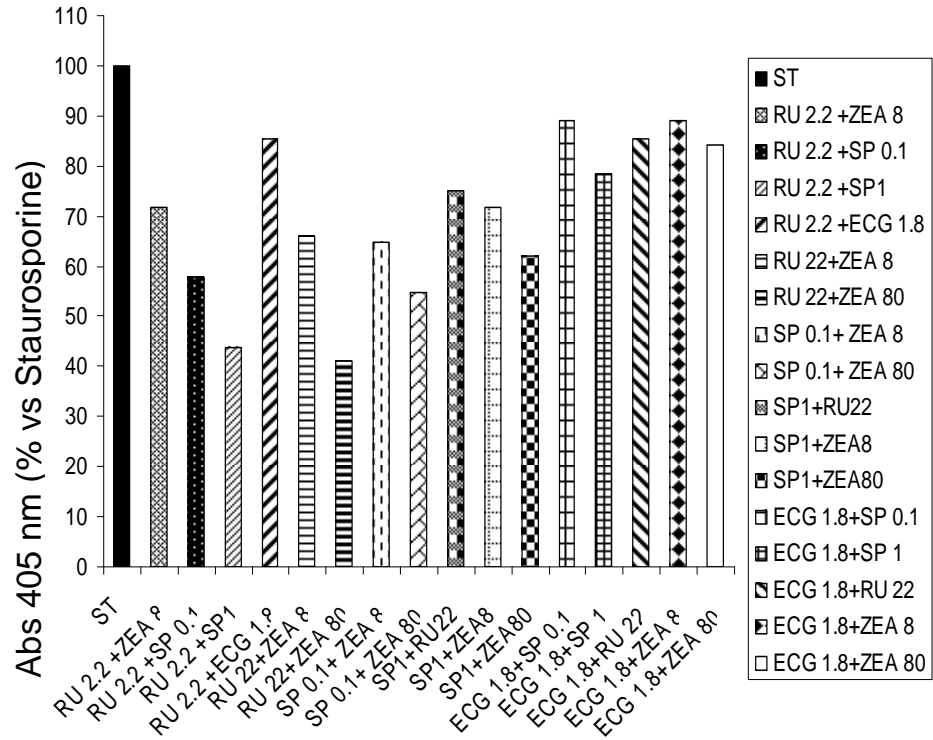
The active principles were added to the culture medium alone (figure 15) or in different combinations (figure 17).

Figure 16. Caspase-3 activity reduction by active principles ST staurosporine; SP spermidine; Ru rutin; ZEA zeaxanthin; ECG epigallocatechin gallate



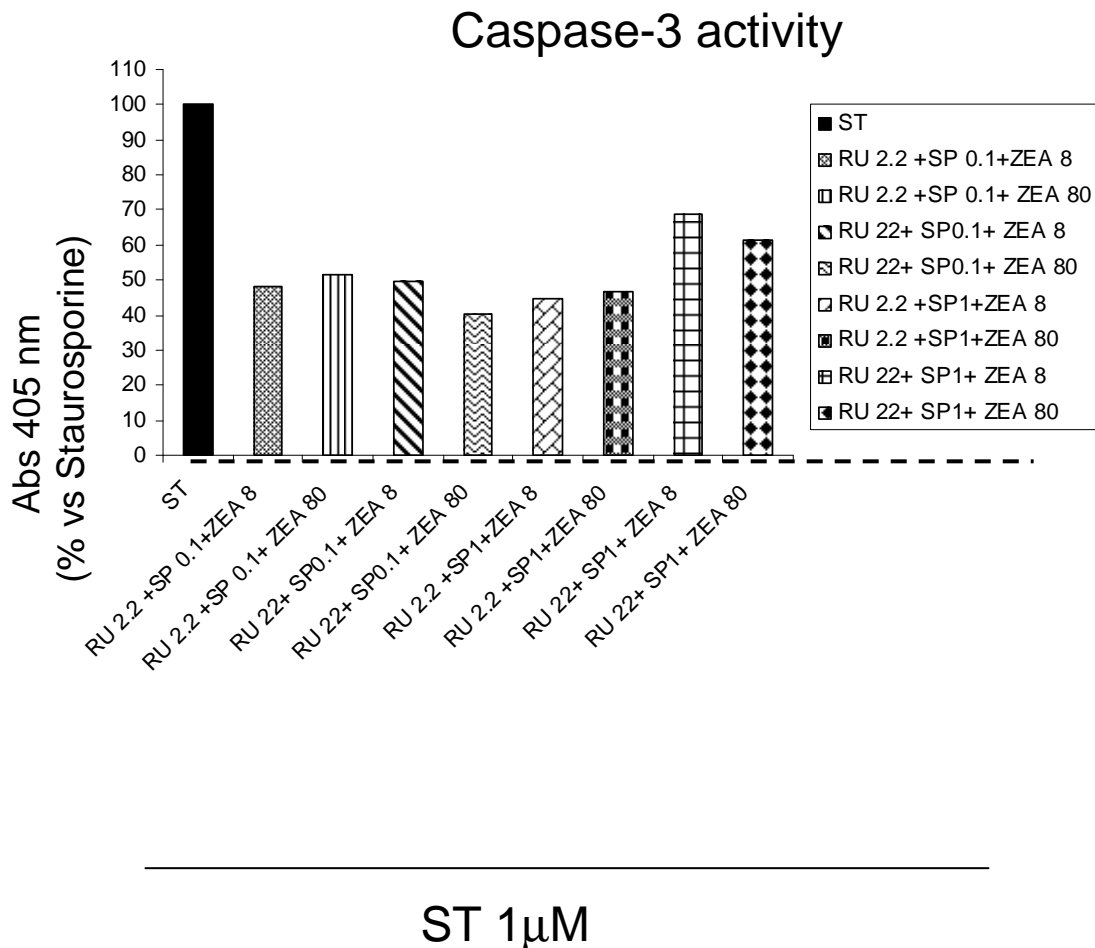
In figure 16 it is shown that Rutin alone at 22 μM concentration reduced by 50% the Staurosporin-induced caspase-3 activity, at the lower concentration the reduction was 35%. At best, Sperimidin (1 μM) alone decreased the enzyme activity by 40% and Zeaxanthin (8 μM) above 30%. The higher zeaxanthin concentration resulted less effective. It was also observed that the addition of epigallocatechin gallate at the final concentration of 18 μM (EGCG 18) to staurosporin had a negative impact on cellular morphology and preservation. After 24 hours cells were broken into pieces. This may explain the lack of Absorbance shown in figure 16.

Figure 17. Caspase-3 activity reduction by different combinations of two anti-apoptotic principles. ST staurosporine; SP spermidine; Ru rutin; ZEA zeaxanthin.



+ ST 1 μ M

Figure 18. Caspase-3 activity reduction by different combinations of three active principles. ST staurosporine; SP spermidine; Ru rutin; ZEA zeaxanthin.



The association of Rutin with Sperimidin (1 μ M) or Zeaxanthin (80 μ M) enhanced its inhibition on the apoptotic process. In particular the addition of spermidin allowed the best inhibition of caspase- 3 activity with Rutin at 2.2 μ M, while the higher concentration of Rutin (22 μ M) was less effective when associated to sperimidin (1 μ M). Also of interest the boosting effect obtained with the addition of 22 μ M Rutin to 80 μ M Zeaxanthin that alone reduced caspase activity by 25% and with Rutin addition its effect increased to 60% reduction.

Table 3. The anti-apoptotic actions of investigated compounds as a single molecule or in different combinations was reported as percent of caspase-3 activity inhibition.

	ACTIVE PRINCIPLES [μM]	CASPASE-3 ACTIVITY (%)
ST 1 μM	//	100
“	SP 0.1	78,36
“	SP 1	63,1
“	RU 2.2	67,9
“	RU 22	53,73
“	ZEA 8	71
“	ZEA 80	86,8
“	EGCG 1.8	101
“	EGCG 18	0
“		
“	RU 2.2 +ZEA 8	71,67
“	RU 2.2 +SP 0.1	57,68++
“	RU 2.2 +SP1	43,68+++
“	RU 2.2 +ECG 1.8	85,32-
“	RU 22+ZEA 8	65,87
“	RU 22+ZEA 80	40,95+++
“	SP 0.1+ ZEA 8	64,84+
“	SP 0.1+ ZEA 80	54,61++
“	SP1+RU22	75,085?
“	SP1+ZEA8	71,67
“	SP1+ZEA80	62,11
“	ECG 1.8+SP 0.1	89,07*
“	ECG 1.8+SP 1	78,5*
“	ECG 1.8+RU 22	85,32*
“	ECG 1.8+ZEA 8	89,078*
“	ECG 1.8+ZEA 80	84,3*
“	RU 2.2+ ZEA 80	54,89+
“	RU 22+SP 0.1	60,14+
“		
“	RU 2.2 +SP 0.1+ZEA 8	48,25
“	RU 2.2 +SP 0.1+ ZEA 80	51,7
“	RU 22+ SP0.1+ ZEA 8	49,6++
“	RU 22+ SP0.1 + ZEA 80	40,21 ++
“	RU 2.2 +SP1+ZEA 8	44,7
“	RU 2.2 +SP1+ZEA 80	46,8
“	RU 22 +SP1+ZEA 8	68,53
“	RU 22 +SP1+ZEA 80	61,53

4.2 Morphological and biochemical evaluation of the anti-apoptotic action of the three active principles

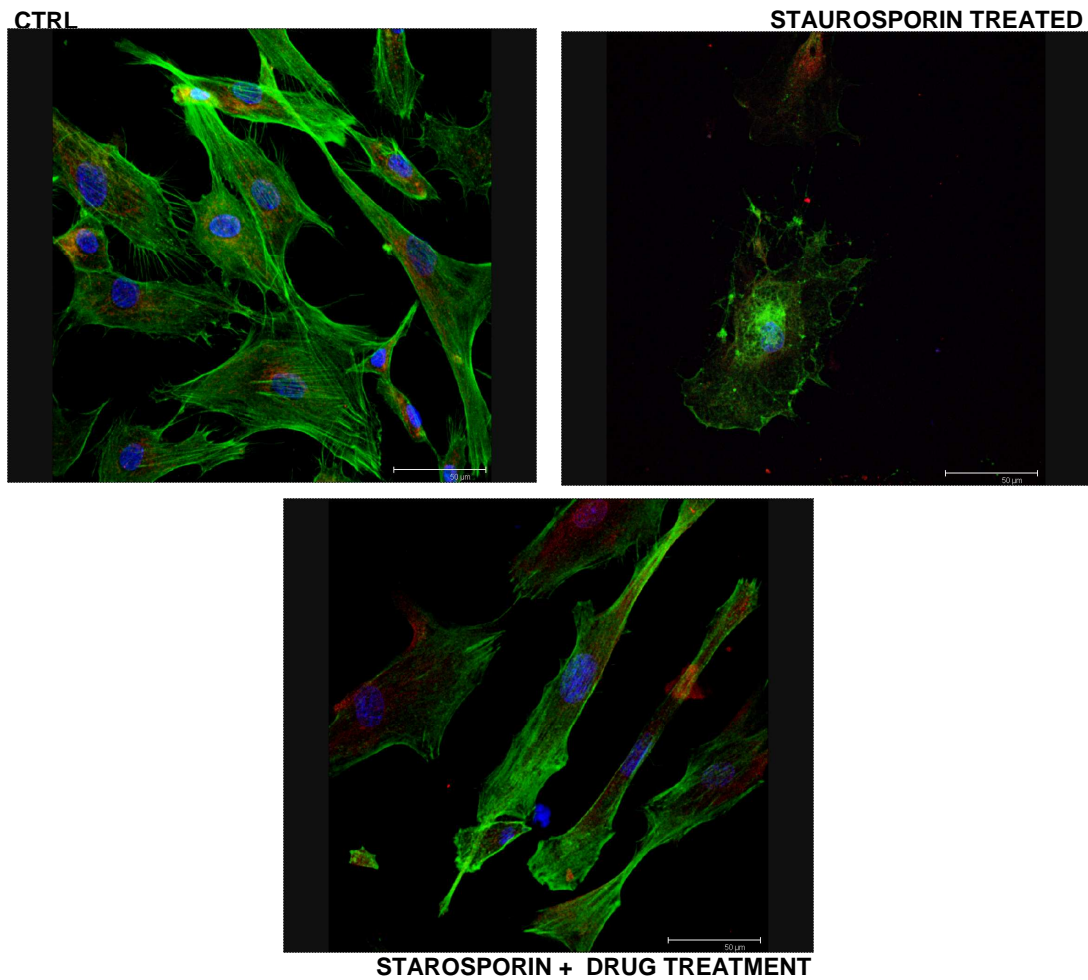
The actions of spermidine, rutin and zeaxanthin in counteracting apoptosis induced by staurosporin was also investigated by means of immunocytochemistry and western blot analyses.

HFDP cells are flat and with different morphologies. The actin cytoskeleton (phalloidin) is distributed through the cell, while ketain-18 is more concentrated around cell nucleus (figure 19).

The staurosporin exposure resulted in a marked activation of Caspase-3 accompanied by cytoskeletal degradation, nuclear blebbing, and cellular fragmentation (Fig. 19 panel A and B). Such a cellular destruction is totally prevented by the combined treatment (SP 0.5 mg/cps; RU 2.5 mg/cps; ZEA 2 mg/cps). The extent of cell loss was greatly reduced, and, differently from untreated cells, there was a total preservation and normal distribution of actin-tubulin cytoskeleton with normal cellular shape, as evidenced by the labelling with phalloindin . Caspase-3 is normally present around the nucleus, and is increased throughout the cell after staurosporin exposure (figure 19B). Following co-administration of Staurosporin and combined treatment, the cell loss is reduced and cellular morphology is preserved (figure 19B). It must be noted however that, differently from control, caspase-3 is distributed throughout the cell (figure 19B, ST+ drug treatment).

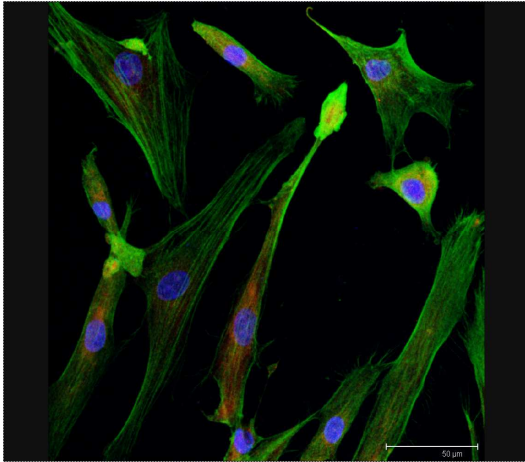
Figure 19. HPDF cellular morphology and apoptosis. A) Red= keratine 8-18; Green= phalloidin; Blue= DAPI; B) Red= caspase-3 (total); Green=phalloidin; Blue=DAPI; C) Shape of cells; D) caspase-3 activity measured with the amount of compounds used in the assay.

A: Red= keratine 8-18; Green= phalloidin; Blue= DAPI;

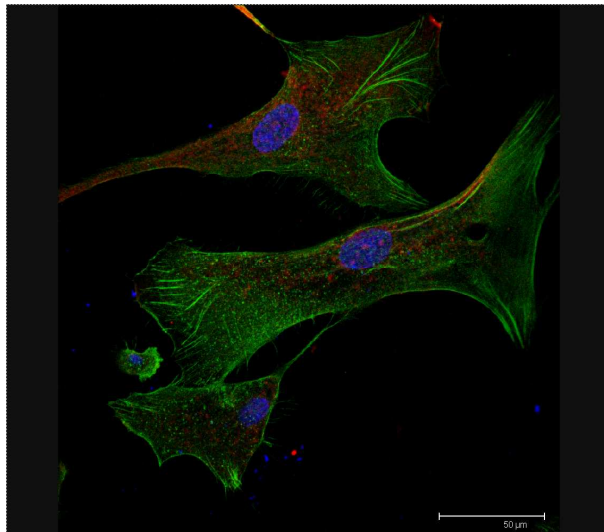
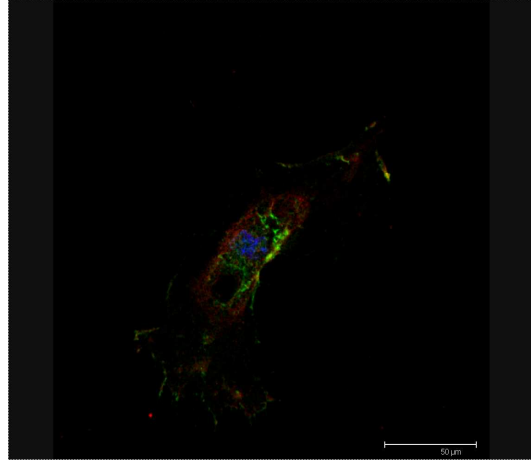


B: Red= caspse-3; Green=phalloidin; Blue=DAPI

CTRL

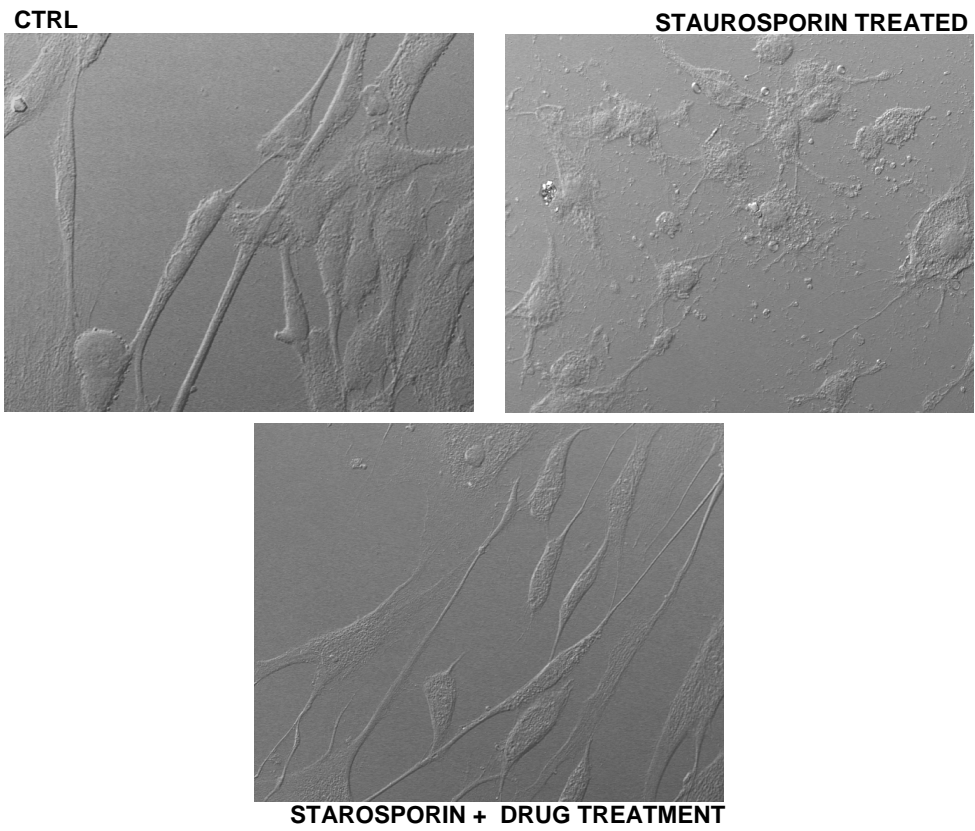


STAUROSPORIN TREATED

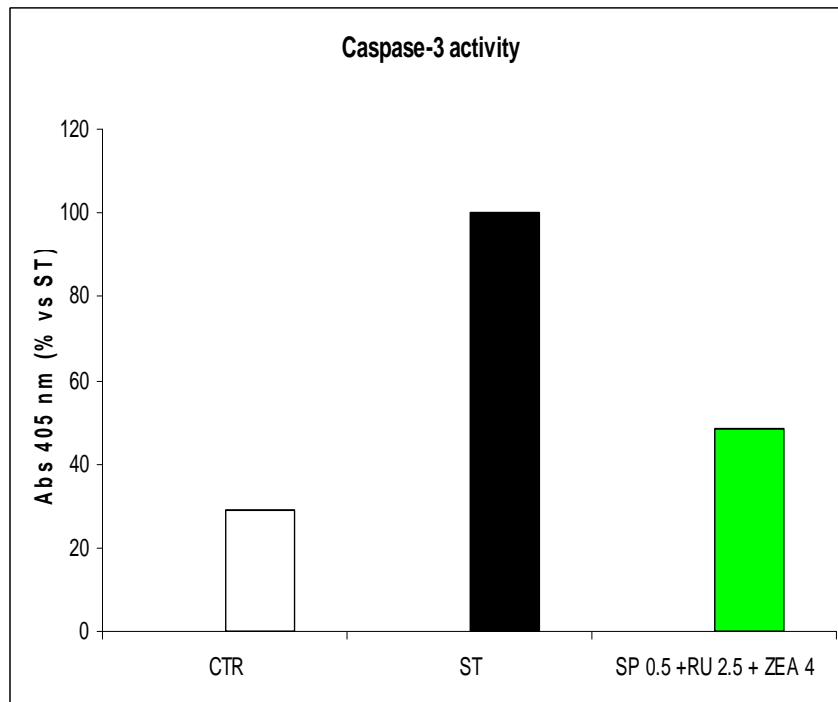


STAROSPORIN + DRUG TREATMENT

C)



D)



The interference microscopy (figure 19C) shows that the few viable cells treated with staurosporin are atrophic, with poor cytoplasm around the nucleus and large vacuolarization. Treatment with the active principles counteracts staurosporin action and maintains the cellular shape and reduces markedly the vacuolarization. In figure 17 D it is shown how staurosporin increased caspase-3 activity by 5 fold and that the chosen treatment is able to reduce it by 75%.

The inhibition of apoptosis was also investigated by western blotting (figure 19A and 19 B) throughout the evaluation of the effect of drug treatment on caspase-3 and Poly (ADP-ribose) polymerase (PARP), a protein involved in a number of cellular processes of DNA repair and programmed cell death. Upon DNA cleavage by enzymes involved in cell death (such as caspases), PARP can deplete cellular ATP in an attempt to repair the damaged DNA. ATP depletion in a cell leads to lysis and cell death.

HFDP cells exposure to staurosporin for 24 hours induced the expression of caspase-3. The increase was about three fold above the control, also PARP expression resulted largely induced (figure 19 A and 19 B). The treatment with two different combinations of SP, RU and ZEA significantly counteracted the effect of staurosporin inhibiting the expression of both capsase-3 and PARP (figure 19 A and 19 B).

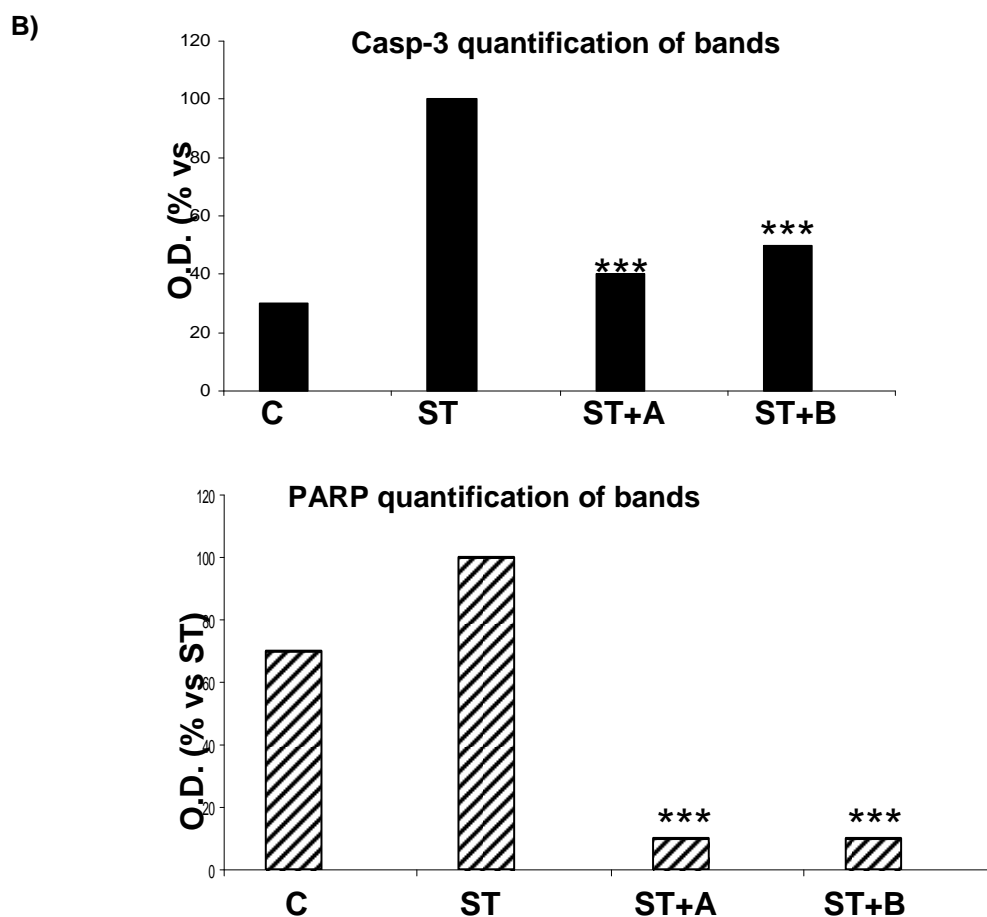
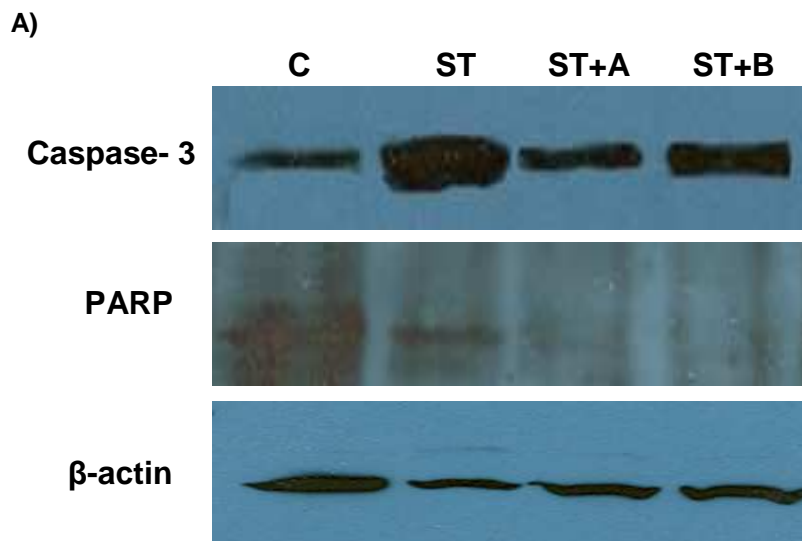
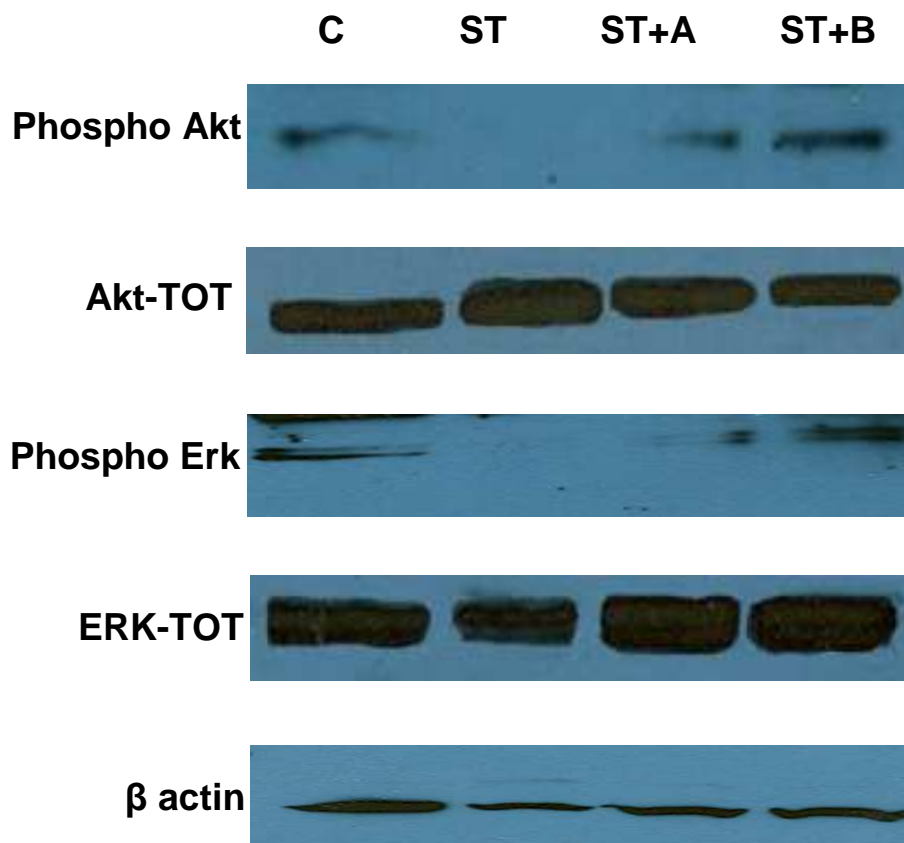


Figure 20. Expression of caspase-3 and PARP. A) The expression of the proteins was evaluated by western blotting using specific polyclonal antibodies; B) quantification of bands reporting the optical density (O.D.) expressed as percent of staurosporin treatment. A = SP 0.5 mg/cps; RU 2.5 mg/cps; ZEA 2 mg/cps B = SP 0.5 mg/cps; RU 2.5 mg/cps; ZEA 4 mg/cps

The efficacy of the drug treatment on apoptosis is further supported by the evaluation of the activity of Akt and MAP kinases ERK1/2 (figure 21 panel A and B), that resulted significantly impaired after cell incubation for 24 hours with staurosporin. The phosphorylated form of both Akt and ERK_{1/2} is greatly reduced by staurosporin, while the enzyme expression is unaffected. The two drug-combinations resulted in the full preservation of the phosphorylated forms, with no changes in enzyme expression.

A)



B

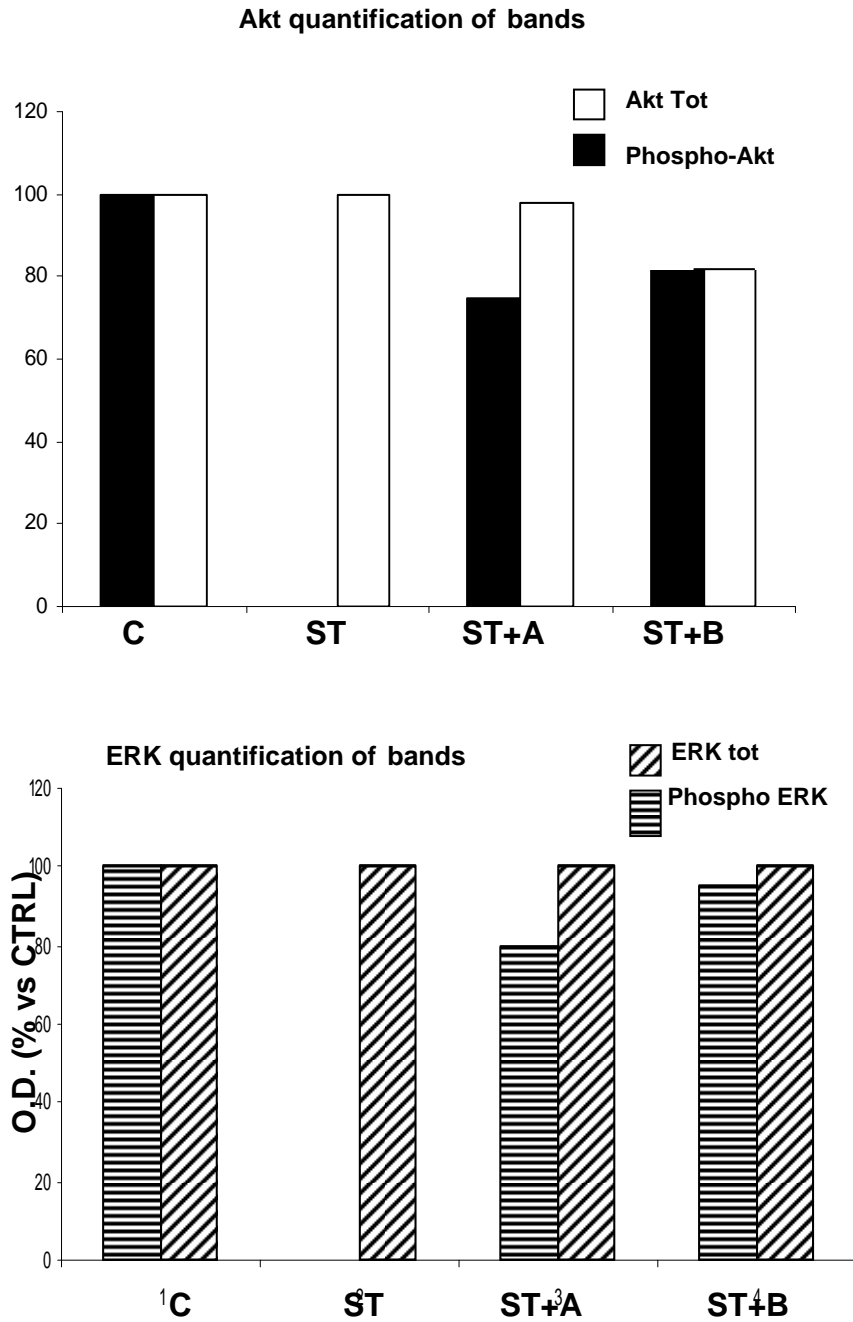


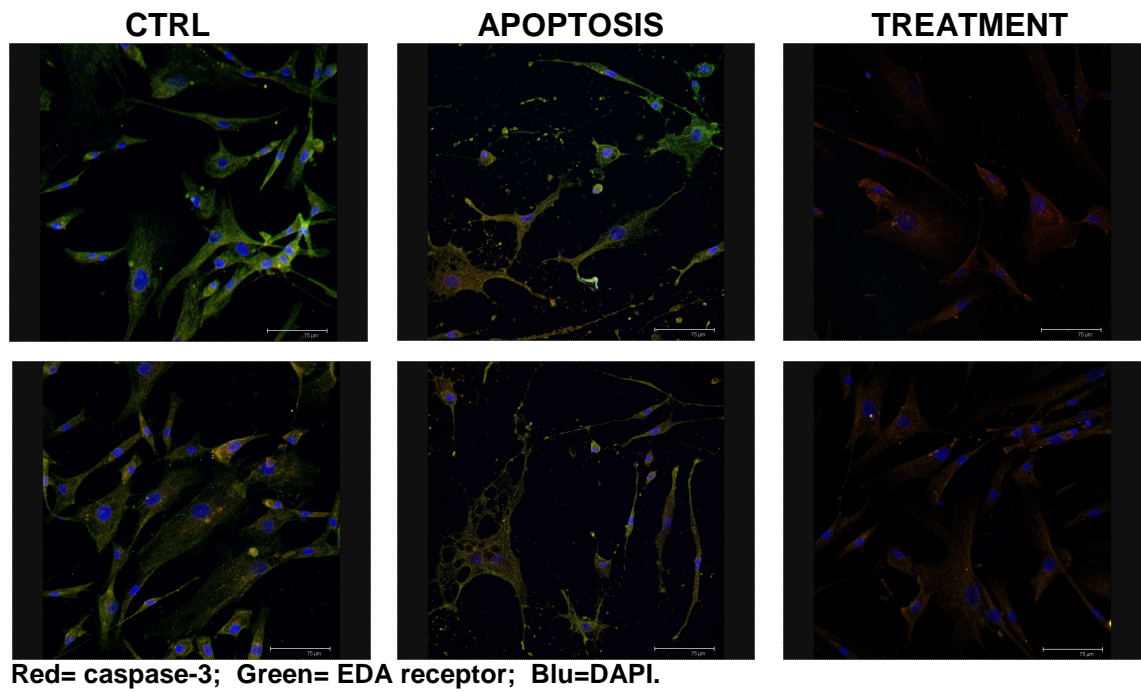
Figure 21. Maintenance of Akt and ERK phosphorylation. A) The expression of the proteins was evaluated by western blotting using specific polyclonal antibodies; B) quantification of bands reporting the optical density (O.D.) expressed as percent of control (CTRL). A = SP 0.5 mg/cps; RU 2.5 mg/cps; ZEA 2 mg/cps B = SP 0.5 mg/cps; RU 2.5 mg/cps; ZEA 4 mg/cps.

4.3 Investigation of EDA-A1/EDAR expression

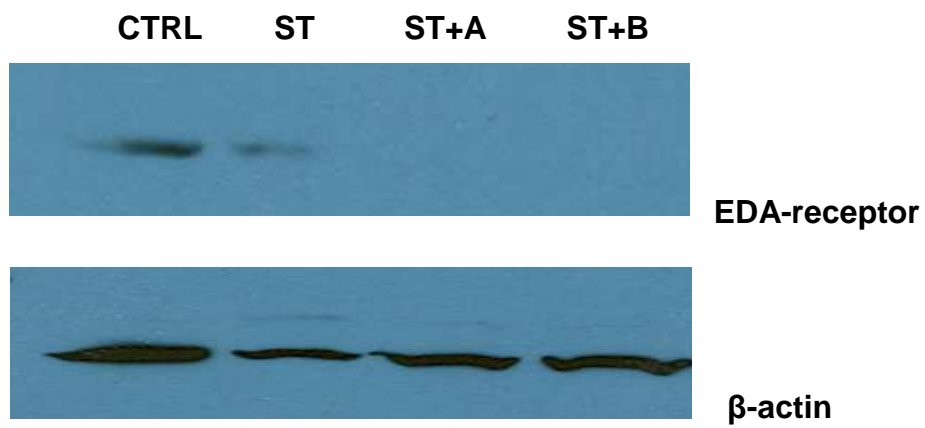
Two receptors for *EDA*, *EDAR* and *EDA2R*, are specific for the two isoforms *EDA-A1* and *EDA-A2*, respectively. *EDA-A1* and its receptor *EDAR* are capable of activating the *NF-kB* pathway and are implicated in hair growth. *EDA2R* is capable of activating the *NF-kB* pathway and also through *TRAF3,6*, *JNK* (c-Jun N-terminal kinase), which activates *c-Jun*. Mutations in *EDA* and *EDAR* give rise to ectodermal dysplasia, a clinical syndrome characterized by loss of hair, sweat glands, and teeth, whereas mutations in *EDA2R* do not. *EDA2R* could influence the onset of AGA through the activation of the *NF-kB* pathway or by *c-Jun*, which has been shown to be critical for *Androgenetic Receptor* transactivation. The expression of *EDAR* was investigated by means of both immunocytochemistry and western blotting analyses. While the expression of *EDA* was studied only by immunocytochemistry. Both methods show that *EDAR* expression in HFDP cells is reduced by apoptosis and much more by drug treatment. Differently, *EDA* expression is increased by staurosporin exposure and is abolished by drug treatment.

Figure 22. EDAR expression.

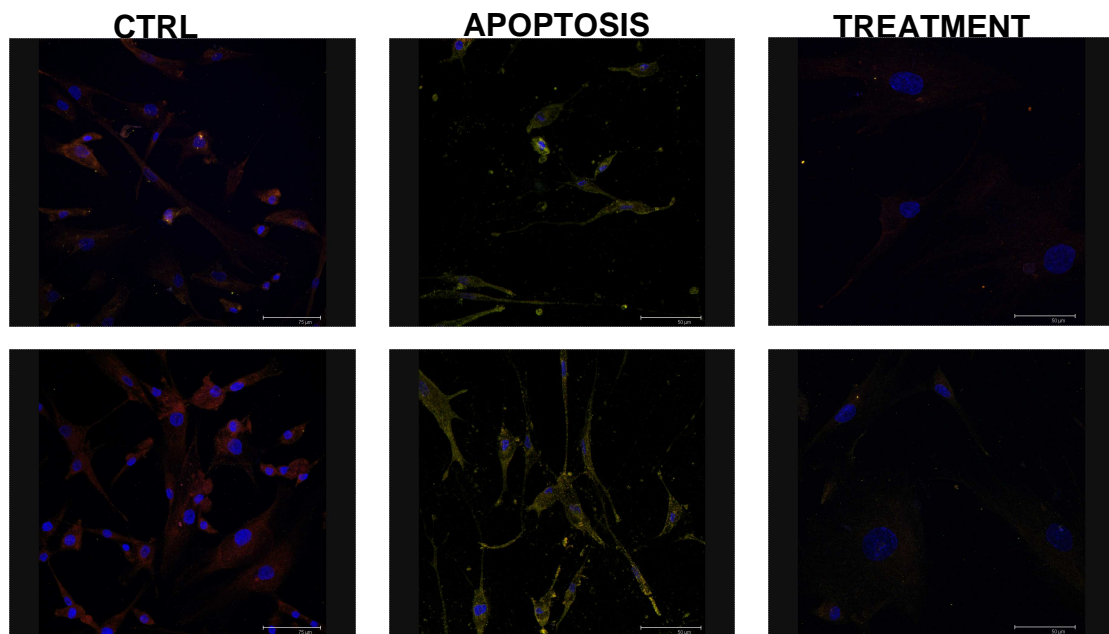
A)



B)



c)



Red= caspase-3; Green= EDA1; Blu=DAPI

Figure22. EDAR/EDA1 expression. A) The expression of the proteins was evaluated by western blotting using specific polyclonal antibodies. The treatment used in the immunofluorescence is referred to the incubation of mixture A. We obtained the same results with the mixture B. A = SP 0.5 mg/cps; RU 2.5 mg/cps; ZEA 2 mg/cps B = SP 0.5 mg/cps; RU 2.5 mg/cps; ZEA 4 mg/cps

4.4 TUNEL assay

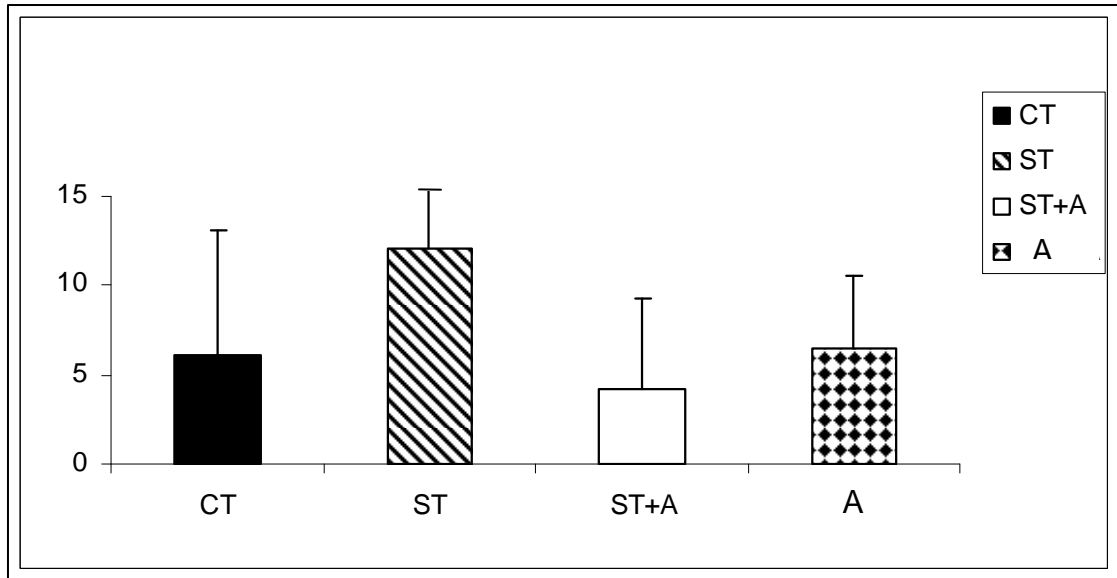


Fig. 23 Quantification of apoptotic cells with The DeadEnd™ Fluorometric TUNEL System
A= Rutin 2,5mg/cps, Spermidine 0,5 mg/cps, Zeaxanthin 2 mg/cps;

The DeadEnd™ Fluorometric TUNEL System was elaborated for the specific detection and quantification of apoptotic cells in a defined cell culture. After fixing cells with paraphormaldeid we performed Fluorimetric assay, counted apoptotic cells (green) and total cells in each box, and we made the statistical analysis. The higher percentage of apoptotic cells is present in staurosporin-treated group. As it is shown in figure 23, the number of staurosporin-induced Tunal positive cells is significantly decrease by the treatment.

4.5 HFDP cells proliferation

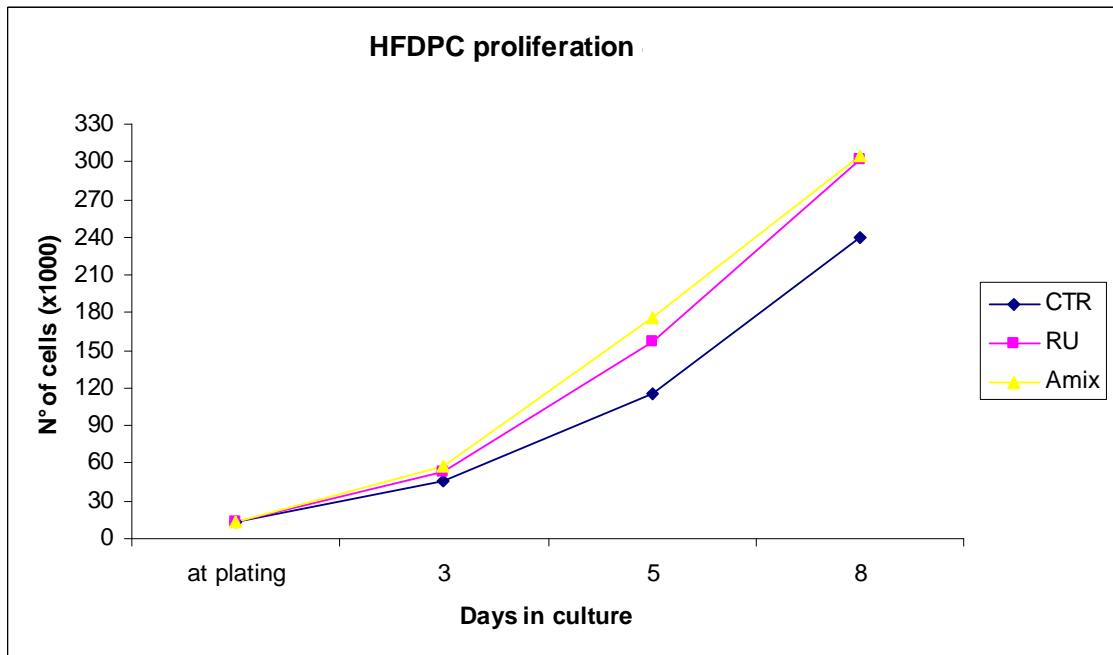
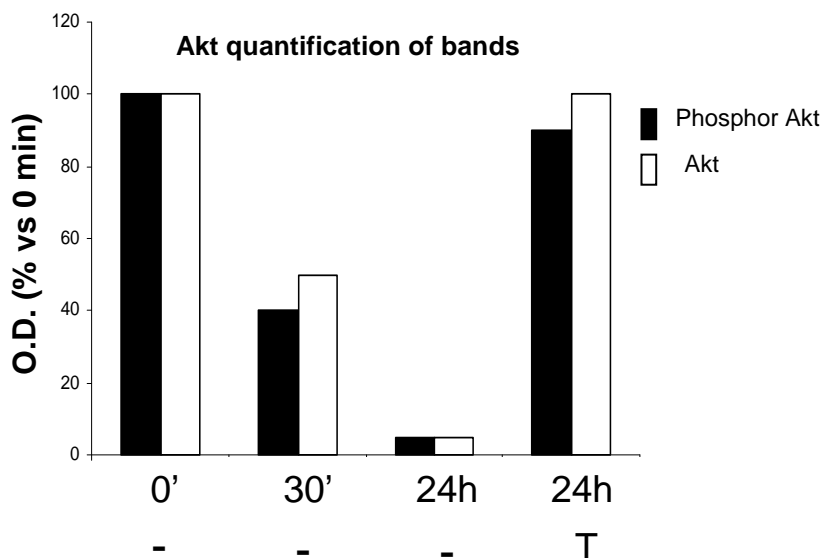
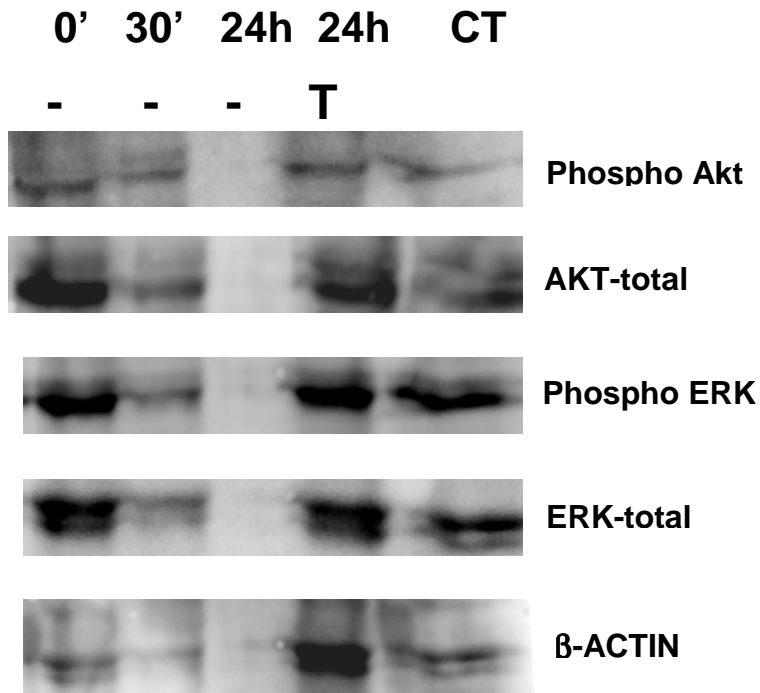


Fig. 24 Proliferation curve of HFDP cells after 3,5 and 8 days. A= Rutin 2,5mg/cps, Spermidine 0,5 mg/cps, Zeaxanthin 2 mg/cps.

We also tested this three active principles on cells proliferation. Results are shown in figure 24, cells are treated with the mixture of rutin, spermidine and zeaxanthin, and also by rutin alone. At three days the number of treated cells is comparable among treated and no-treated ones. At 5 days a clear difference among the three groups can be noticed. Treated cells are an higher number suggesting an effect of these agents on proliferation. After 8 days the number of non treated cells is definitely lower than the others. Rutin appears as effective as the mixture in enhancing HFDP cells proliferation.

4.6 Prevention of protein degradation in ex-vivo hair bulbs

Incubation at 37°C (t)



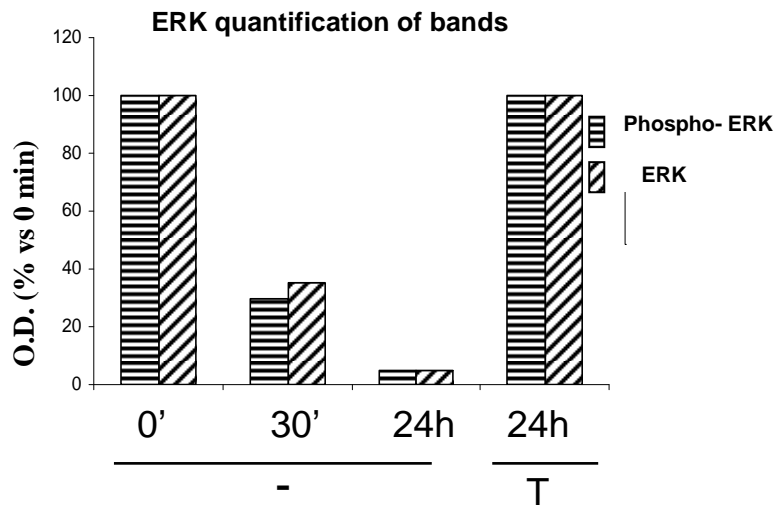
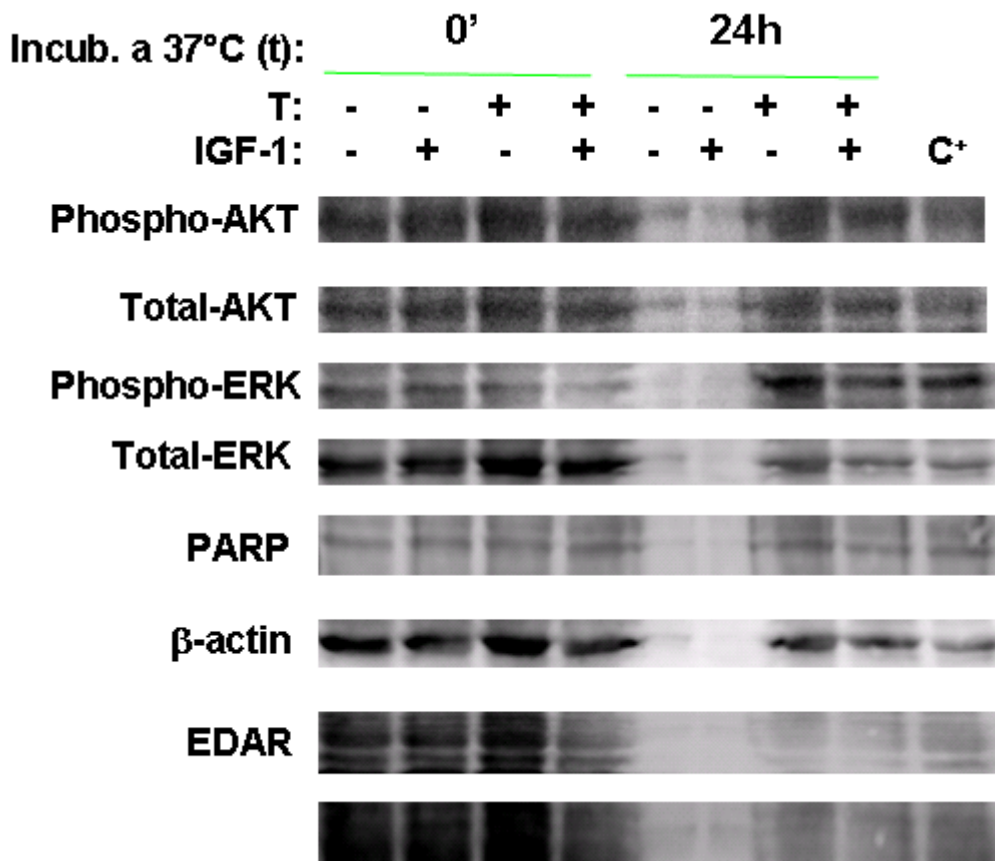


Figure 25. Prevention of protein degradation in ex-vivo bulbs. A) The expression of the proteins was evaluated by western blotting using specific polyclonal antibodies. B) quantification of bands reporting the optical density (O.D.) expressed as percent of control (0').

Ex-vivo human hair bulbs were incubated for 24 hours in cells culture medium at 37°C. After 24 hours hair were homogenised and processed for western blotting evaluation of the expression and function of key cellular proteins such as AKT and ERK. The incubative period caused the degradation of both phosphorylated and basal forms of AKT and ERK (Fig. 25). The addition to the incubation medium of the mixture led to the complete preservation of both proteins in basal and phosphorylated forms. The degradation was observed also for actin, that was fully maintained by the treatment.



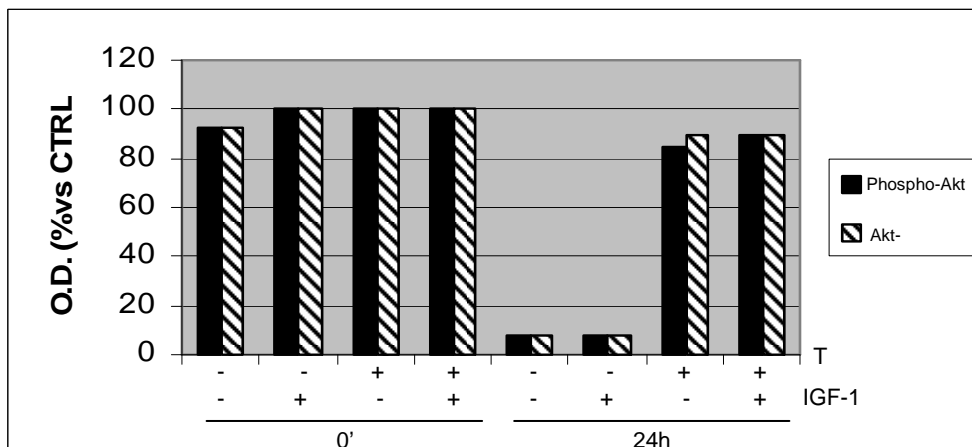
- = Control

IGF-1= 50 ng/ml

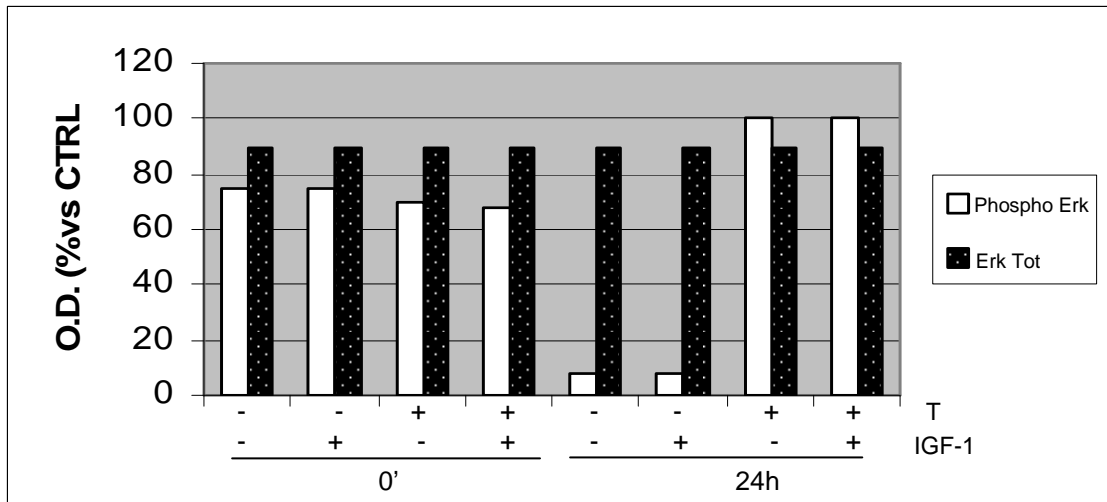
T= Rutin 2,5mg/cps, Spermidine 0,5 mg/cps, Zeaxanthin 2 mg/cps;

C+= protein extract from A549 cells, used as a positive control

Akt quantification of bands



ERK quantification of bands



PARP quantification of bands

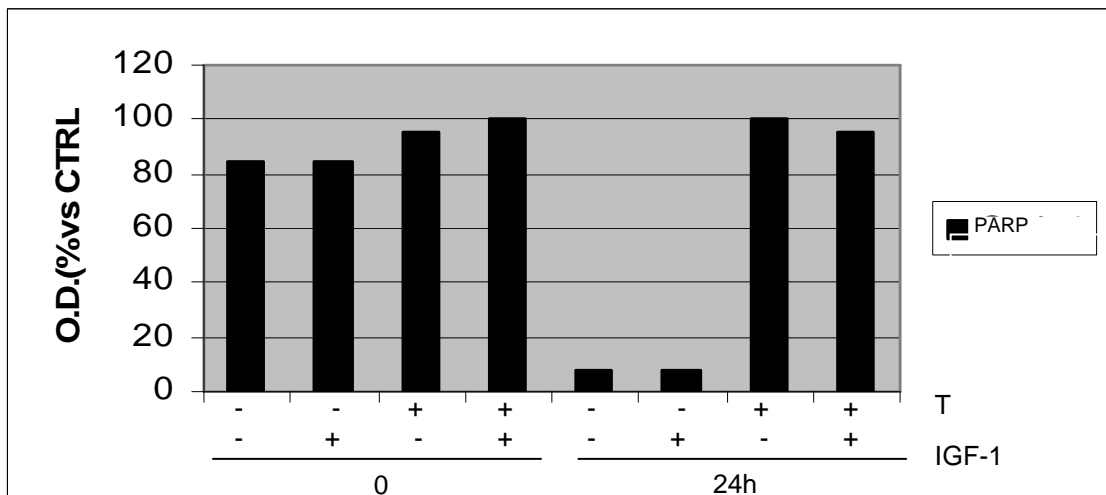


Figure 26. Prevention of protein degradation in ex-vivo bulbs (2° experiment). A) The expression of the proteins was evaluated by western blotting using specific polyclonal antibodies. B) quantification of bands reporting the optical density (O.D.) expressed as percent of control (0').

Exposure of hair bulbs to IGF-1 enhances phosphorylation of AKT and slightly also ERK. Following 24 hours incubation, bulbs do not show any more detectable amounts of AKT, ERK, and PARP. However the presence of the mixture prevents such a drop in protein content and re-establish the IGF-1 dependent phosphorylation of AKT.

5. Discussion

Androgenetic alopecia is a genetically determined disorder and is progressive through the gradual conversion of terminal hairs into indeterminate hairs and finally to vellus hairs. [Osborn]. Patients with androgenetic alopecia have a reduction in the terminal-to-vellus hair ratio, normally about 4:1. Following miniaturization of the follicles, fibrous tracts remain. Patients with this disorder usually have a typical patterned distribution of hair loss. [Otberg et al.]. The onset of androgenetic alopecia is gradual. Men present with gradual thinning in the temporal areas, producing a reshaping of the anterior part of the hairline. For the most part, the evolution of baldness progresses according to the Norwood/Hamilton [Norwood et al.] classification of frontal and vertex thinning. Women with androgenetic alopecia usually present with diffuse thinning on the crown. Bitemporal recession does occur in women but usually to a lesser degree than in men. In general, women maintain a frontal hairline.

Androgenetic alopecia is essentially a cosmetic disorder, other than affecting the patient psychologically [Cash; Stough et al.].

Cycling of hair follicles in the mouse has been intensively investigated from the histological and molecular viewpoints. It is clear that the mammalian hair follicle is an extremely complex organ that undergoes periods of growth (anagen), involution (catagen), and quiescence (telogen) [Courtois et al.]. Mediators suspected of dictating the cyclic action of the follicles in the murine model include dozens of biochemicals that have been studied in other cell signaling pathways, including those involved with the initiation of apoptosis or programmed cell death [Weinberg et al.]. In 1997, Lindner et al mapped the expression of biochemical mediators throughout the follicular cycle of mice,

demonstrating the complex association of biochemical signaling with follicular phase changes [Lindner et al.].

The mesenchyme-derived dermal papilla plays a major regulatory role in the complex cell biology of the hair follicle. The ability to culture dermal papilla cells from a range of species and particularly a range of normal and disordered human hair follicles has enabled the development of a powerful new model system for investigating hair follicle biology. Already these studies have reinforced the importance of dermal papilla cells in initiating new follicle growth and in androgen action in human hair follicles [Oliver et al.]. The retention of hair growth inducing capabilities and characteristics that reflect their in vivo responsiveness to androgens in culture means that they offer a potentially useful approach despite significant drawbacks in working with the cells themselves [Ohtsuki et al.]. Further studies using dermal papilla cells may well elucidate key molecules involved in hair biology in health and disease and, thereby, lead to better therapeutic regimens [Randall].

Research in and around apoptosis has increased substantially since the early 1990s. In addition to its importance as a biological phenomenon, defective apoptotic processes have been implicated in an extensive variety of diseases.

Sequential activation of caspases plays a central role in the execution-phase of cell apoptosis. Caspases exist as inactive proenzymes that undergo proteolytic processing at conserved aspartic residues to produce two subunits, large and small, that dimerize to form the active enzyme. A member of this family, caspase-3 (CPP32, apopain, YAMA) has been identified as being a key mediator of apoptosis of mammalian cells [Kothakota et al.]. Our study was

mostly focused on the activity of this enzyme. Its activity was measured by a specific assay.

The experiment was firstly run testing 4 different non synthetic molecules and measuring the activity of the enzyme when Staurosporin 1 microM was added to the cells. The strongest effect was after 24 hours and it could produce an effect very close to catagen. By reproducing a natural effect in our cells we tested the principles.

Epigallocatechin gallate was excluded at the beginning of the job. Its action did not inhibit the activity caspase-3.

Spermidine and rutin, utilized as single active principle are the most affective compounds capable of inhibiting the increase of caspase-3 activity induced by staurosporin. Rutin at the concentration of 22 μ M (RU 22) reduced caspase-3 activation by about 50%. Many combinations of two compounds resulted to be much more effective, than the compounds alone, in the inhibition of caspase-3 activity (underlined in yellow in the summary table). In particular the combinations RU2.2 + SP1, RU22 + ZEA80 e SP 0.1 + ZEA 80 reduced the activity of caspase-3 by 60%.

When the combination contained the three active principles, we observed an action by promoting zeaxanthin (in green in summary table), that as single agent was not particularly effective. Zeaxanthin, when added to the combination of RU+SP, ameliorated the action of the two drugs co-administrated.

The inhibition of caspase-3 activity is associated to a reduced enhancement of caspase-3 expression by staurosporin treatment. Apoptosis as a different course. Morphologically the protective effects of drugs was even more

remarkable, as staurosporin caused cellular blebbing and destruction. Drug exposure protected HFDP cells allowing the maintenance of normal cytoskeletal cellular structure.

In treated cells phalloidin one of cytoskeleton markers is still visible, where in apoptotic cells is mostly disappeared; it means that the regular shape is kept, compared to the control one. Also the structure of the cytokeratin Keratin 8-18 is still visible where in apoptotic cells is less. As we can see in images the treated cells shape is very close to the control ones.

Tunnel assay, a specific assay to remark apoptosis, shows that apoptosis is strongly reduced in treated cells.

The result we obtained, using the three principles without staurosporin, is that its action is not only apoptosis dependent but it can also play a key role in cellular growing and differentiation.

We may conclude that array of in-vitro and ex-vivo evidences show the effectiveness of these active principles in preventing hair bulb cellular apoptosis and in maintaining expression and function of key enzymes such as Akt and MAP kinases.

6. Bibliography

Ahouansou S, Le Toumelin P, Crickx B, Descamps V. Association of androgenetic alopecia and hypertension. *Eur J Dermatol*. May-Jun 2007;17(3):220-2..

Almeida JS, Lima F, Ros SD, Bulhões LO, de Carvalho LM, Beck RC Nanostructured Systems Containing Rutin: In Vitro Antioxidant Activity and Photostability Studies. *Nanoscale Res Lett*. 2010 Jul 15;5(10):1603-1610.

Andl T, et al., Wnt Signals are required for the initiation of hair follicle development, *Developmental Cells* 2, 643-653.

Ashton-Beaucage D, Therrien M. The greater RTK/RAS/ERK signalling pathway: how genetics has helped piece together a signalling network. *Med Sci (Paris)*. 2010 Dec;26(12):1067-1073

Betin V.M.S. and Lane, J.D. (2007). The cytoskeleton and the control of organelle dynamics in the apoptotic execution phase. *SEB Symposium Series* 59, 267-289.

Botchkarev VA, Kishimoto J. Molecular control of epithelial-mesenchymal interactions during hair follicle cycling. *J Invest Dermatol Symp Proc* 2003; 8: 46–55.

Brouard M, Barrandon Y. Controlling skin morphogenesis. hope and despair. *Curr Opi Biotech* 2003; 14: 520–5.

Bucheli P, Vidal K, Shen L, Gu Z, Zhang C, Miller LE, Wang. Goji Berry Effects on Macular Characteristics and Plasma Antioxidant Levels. *J. Optom Vis Sci*. 2010 Dec 16.

Cash, T.F. (1992) The psychological effects of androgenetic alopecia in men. *J Am Acad Dermatol* 26, 926-931

Chen QP, Giannobile WV. Adenoviral gene transfer of PDGF downregulates gas gene product PDGFalphaR and prolongs ERK and Akt/PKB activation. *Am J Physiol Cell Physiol*. 2002 Mar;282(3):C538-44.

Chen T, Wong YS. Selenocystine induces S-phase arrest and apoptosis in human breast adenocarcinoma MCF-7 cells by modulating ERK and Akt phosphorylation. *J Agric Food Chem*. 2008 Nov 26;56(22):10574-81.

Coleman M.L, Sahai E.A., Yeo M., Bosch M., Dewar A. and Olson M.F. (2001). Membrane blebbing during apoptosis results from caspase-mediated activation of ROCK I. *Nat. Cell Biol.* 3, 339-345.

Courtois, M. et al. (1994) Hair cycle and alopecia. *Skin Pharmacol* 7, 84-89.

Cui Ch. Yi et al., Ectodysplasin regulates the lymphotoxin- β pathway for hair differentiation, *PNAS* 103, 9142-9147.

Earnshaw W.C, Martins L.M. and Kaufmann S.H. (1999). Mammalian caspases: structure, activation, substrates, and functions during apoptosis. *Annu. Rev. Biochem.* 68, 383-424.

El-Mowafy AM, Al-Gayyar MM, Salem HA, El-Mesery ME, Darweish MM. Novel chemotherapeutic and renal protective effects for the green tea (EGCG): role of oxidative stress and inflammatory-cytokine signaling. *Phytomedicine*. 2010 Dec 1;17(14):1067-75. Epub 2010 Sep 18.

Ellis J.A, Stebbing, M. and Harrap, S.B. (2001) Male pattern baldness is not associated with established cardiovascular risk factors in the general population. *Clin Sci (Lond)* 100, 401-404.

Fan TJ, Han LH, Cong RS, Liang J. Caspase family proteases and apoptosis. *Acta Biochim Biophys Sin (Shanghai)*. 2005 Nov;37(11):719-27.

Ferri K.F. and Kroemer G. (2001). Organelle-specific initiation of cell death pathways. *Nat. Cell Biol.* 3, E255-263.

Fessing M. Y. et al., Involvement of the Edar signalling in the control of hair follicle involution (catagen), *The American Journal of Pathology* 169, 2075-2084.

Fonseca YM, Catini CD, Vicentini FT, Cardoso JC, Cavalcanti De Albuquerque Junior RL, Vieira Fonseca MJ. Efficacy of marigold extract-loaded formulations against UV-induced oxidative stress. *J Pharm Sci.* 2010 Dec 23.

Gambardella L, Barrandon Y. The multifaceted adult epidermal stem cell. *Cur Opin Cell Biol* 2003; 15: 771–7.

García-Faroldi G, Rodríguez CE, Urdiales JL, Pérez-Pomares JM, Dávila JC, Pejler G, Sánchez-Jiménez F, Fajardo I. Polyamines are present in mast cell secretory granules and are important for granule homeostasis. *PLoS One*. 2010 Nov 30;5(11):e15071.

Gedaly R, Angulo P, Hundley J, Daily MF, Chen C, Koch A, Evers BMPI-103 and Sorafenib Inhibit Hepatocellular Carcinoma Cell Proliferation by Blocking Ras/Raf/MAPK and PI3K/AKT/mTOR Pathways. *Anticancer Res.* 2010 Dec;30(12):4951-8.

Gong G, Qin Y, Huang W, Zhou S, Yang X, Li D. Rutin inhibits hydrogen peroxide-induced apoptosis through regulating reactive oxygen species mediated mitochondrial dysfunction pathway in human umbilical vein endothelial cells. *Eur J Pharmacol.* 2010 Feb 25;628(1-3):27-35.

Hamilton JB. Patterned loss of hair in man; types and incidence. *Ann N Y Acad Sci.* Mar 1951;53(3):708-28.

Hammerschmidt B, et al., Localization of Shh expression by Wnt and Eda affects axial polarity and shape of hairs, *Development Biology* 305, 246-261.

Hawk E, Breslow, R.A. and Graubard, B.I. (2000) Male pattern baldness and clinical prostate cancer in the epidemiologic follow-up of the first National Health and Nutrition Examination Survey. *Cancer Epidemiol Biomarkers Prev* 9, 523-527.

Janne O.A. et al. (1993) Androgen receptor and mechanism of androgen action. *Ann Med* 25, 83-89.

Ji HF. Insight into the strong antioxidant activity of deinoxanthin, a unique carotenoid in *deinococcus radiodurans*. *Int J Mol Sci*. 2010 Nov 10;11(11):4506-10

Julien LA, Roux PP. mTOR, the mammalian target of rapamycin. *Med Sci (Paris)*. 2010 Dec;26(12):1056-1060.

Kaufman KD. Androgen metabolism as it affects hair growth in androgenetic alopecia. *Dermatol Clin*. Oct 1996;14(4):697-711.

Kligman, A. (1959) The human hair cycle. *J Invest Dermatol* 33, 307-316

Kothakota S et al: Caspase 3-generated fragment of gelsolin: effector of morphological change in apoptosis. *Science* 278, 294-298, 1997

Kuida K, Haydar T.F., Kuan C.Y., Gu Y., Taya C., Karasuyama H., Su M.S., Rakic P. and Flavell R.A. (1998). Reduced apoptosis and cytochrome c-mediated caspase activation in mice lacking caspase 9. *Cell* 94, 325-337.

Kwack M. H. et al., Dihydrotestosterone-inducible Dickkopf 1 from Balding Dermal Papilla Cells causes apoptosis in follicular keratinocytes, *The Journal of Investigative Dermatology* 128, 262-269.

Lane J.D, Allan V.J. and Woodman P.G. (2005). Active relocation of chromatin and endoplasmic reticulum into blebs in late apoptotic cells. *J. Cell Sci*. 118, 4059-4071.

Langbein L. et al., Expression of the nine type 1 members in the hair follicle, *The Journal of Biological Chemistry* 28, 19874-19884.

Laurikkala J. et al., Regulation of hair follicle development by the TNF signal ectodysplasin and its receptor Edar, *Development* 129, 2541-2553.

Lecerf JM, Desmettre T. Nutrition and age-related macular degeneration. *J Fr Ophthalmol*. 2010 Dec;33(10):749-57.

Lesko SM, Rosenberg L, Shapiro S. A case-control study of baldness in relation to myocardial infarction in men. *JAMA*. Feb 24 1993;269(8):998-1003.

Lindner G, Botchkarev VA, Botchkareva NV, Ling G, van der Veen C, Paus R. Analysis of apoptosis during hair follicle regression (catagen) *Am J Pathol.* 1997 Dec;151(6):1601-17.

Ludwig E. Classification of the types of androgenetic alopecia (common baldness) occurring in the female sex. *Br J Dermatol.* Sep 1977;97(3):247-54.

Matsuzaki T, Yoshizato K. Role of hair papilla cells on induction and regeneration processes of hair follicle. *Wound Repair Regen* 1998; 6: 524–30.

McElwee KJ, Kissling S, Wenzel E et al. Cultured peribulbar dermal sheath cells can induce hair follicle development and contribute to the dermal sheath and dermal papilla. *J Invest Dermatol* 2003; 121: 1267–75.

Midorikawa T. et al., Different gene expression profile observed in dermal papilla cells related to androgenic alopecia by DNA microarray analysis, *Journal of Dermatological Science* 36, 25-32.

Mikkola M. M, et al., Ectodysplasin signalling in development, *Cytokine & Growth Factor Reviews* 14, 211-224.

Mikkola M. M, TNF superfamily in skin appendage development, *Cytokine & Growth Factor Reviews* 19, 219-230.

Millar SE. Molecular mechanisms regulating hair follicle development. *J Invest Dermatol* 2002; 118: 216–25.

Mills J.C, Stone N.L. and Pittman R.N. (1999). Extranuclear apoptosis. The role of the cytoplasm in the execution phase. *J. Cell Biol.* 146, 703-708.

Monobe M, Ema K, Tokuda Y, Maeda-Yamamoto M. Effect on the Epigallocatechin Gallate/Epigallocatechin Ratio in a Green Tea (*Camellia sinensis* L.) Extract of Different Extraction Temperatures and Its Effect on IgA Production in Mice. *Biosci Biotechnol Biochem.* 2010;74(12):2501-3

Moss D.K. and Lane J.D. (2006). Microtubules: forgotten players in the apoptotic execution phase. *Trends Cell Biol.* 16, 330-338.

Muller SA. Alopecia: syndromes of genetic significance. *J Invest Dermatol.* Jun 1973;60(6):475-92.

Norwood O.T. (1975) Male pattern baldness: classification and incidence. *South Med J* 68, 1359-1365

Oh B.R. et al. (1998) Association of benign prostatic hyperplasia with male pattern baldness. *Urology* 51, 744-748.

Ohtsuki A, Hasegawa T, Ikeda S. Treatment of alopecia areata with 308-nm excimer lamp. *J Dermatol.* 2010 Dec;37(12):1032-1035. doi: 10.1111/j.1346-8138.2010.00942.x. Epub 2010 Sep 29.

Oliver R. and Jahoda, C. (1989) The dermal papilla and the maintenance of hair growth. In *The Biology of Wool and Hair* (Rogers, G. et al, eds), pp. 51-67, Chapman and Hall, London, UK

Olsen EA. Androgenetic alopecia. In: Olsen EA ed. *Disorders of Hair Growth: Diagnosis and Treatment.* New York, NY: McGraw-Hill; 1994:257-83.

Osada A, Iwabuchi T, Kishimoto J et al. Long-term culture of mouse vibrissal dermal papilla cells and de novo hair follicle induction. *Tissue Eng* 2007; 13: 975–82.

Osborn D. (1916) Inheritance of baldness. *J Heredity* 7, 347-355

Otberg N, Finner AM, Shapiro J. Androgenetic alopecia. *Endocrinol Metab Clin North Am.* Jun 2007;36(2):379-98

Prodi D. A. et al., EDA2R is associated with Androgenic Alopecia, *The Journal of Investigative Dermatology* 128, 2268-2270.

Randall V.A. (1996) The use of dermal papilla cells in studies of normal and abnormal hair follicle biology. *Dermatol Clin* 14, 585-594,

Rathnayake D, Sinclair R. Innovative use of spironolactone as an antiandrogen in the treatment of female pattern hair loss. *Dermatol Clin.* 2010 Jul;28(3):611-8.

Rendl M, Lewis L, Fuchs E. Molecular dissection of mesenchymal-epithelial interactions in the hair follicle. *PLoS Biol* 2005; 3: e331.

Richetti SK, Blank M, Capiotti KM, Piato AL, Bogo MR, Vianna MR, Bonan CD. Quercetin and rutin prevent scopolamine-induced memory impairment in zebrafish. *Behav Brain Res.* 2011 Feb 2;217(1):10-5. Epub 2010 Oct 1.

Rocha S, Generalov R, Pereira Mdo C, Peres I, Juzenas P, Coelho MA. Epigallocatechin gallate-loaded polysaccharide nanoparticles for prostate cancer chemoprevention. *Nanomedicine (Lond).* 2011 Jan;6(1):79-87.

Roh C, Tao Q, Lyle S. Dermal papilla-induced hair differentiation of adult epithelial stem cells from human skin. *Physiol Genomics* 2004; 19: 207–17.

Rosenblatt J, Raff M.C. and Cramer L.P. (2001). An epithelial cell destined for apoptosis signals its neighbors to extrude it by an actin and myosin-dependent mechanism. *Curr. Biol.* 11, 1847-1857.

Savill J, Dransfield I., Gregory C., and Haslett C. (2002). A blast from the past: clearance of apoptotic cells regulates immune responses. *Nat. Rev. Immunol.* 2, 965-975.

Schmidt-Ullrich R. et al., *NF- κ B transmits Eda A1/EdaR signalling to activate Shh and cyclin D1 expression, and controls post-initiation hair placode down growth*, *Development* 133, 1045-1057.

Schneider M. R. et al., *The hair follicle as a dynamic miniorgan*, *Current Biology* 19, R132-R142.

Sebbagh M, Renvoize C., Hamelin J., Riche N., Bertoglio J. and Breard J. (2001). *Caspase-3-mediated cleavage of ROCK I induces MLC phosphorylation and apoptotic membrane blebbing*. *Nat. Cell Biol.* 3, 346-352.

Slattum G, McGee K.M. and Rosenblatt J. (2009). *P115 RhoGEF and microtubules decide the direction apoptotic cells extrude from an epithelium*. *J. Cell Biol.* 186, 693-702.

Stenn KS, Cotsarelis G. *Bioengineering the hair follicle: fringe benefits of stem cell technology*. *Curr Opin Biotechnol* 2005; 16: 493–7.

Stough D, Stenn K, Haber R, et al. *Psychological effect, pathophysiology, and management of androgenetic alopecia in men*. *Mayo Clin Proc.* Oct 2005;80(10):1316-22.

Taylor R.C, Cullen S.P. and Martin S.J. (2008). *Apoptosis: controlled demolition at the cellular level*. *Nat. Rev. Mol. Cell Biol.* 9, 231-241.

Trueb RM. *Molecular mechanisms of androgenetic alopecia*. *Exp Gerontol* 2002; 37: 981–90.

Wakisaka N. et al., *Effectiveness of finasteride on patients with male pattern baldness who have different androgen receptor gene polymorphism*, *JID Symposium Proceedings*.

Weger N. et al., *IGF-1 signalling controls the hair growth cycle and the differentiation of hair shafts*, *The Journal of Investigative Dermatology* 125, 873-882.

Weinberg WC, Goodman LV, George C et al. *Reconstitution of hair follicle development in vivo: determination of follicle formation, hair growth, and hair quality by dermal cells*. *J Invest Dermatol* 1993; 100: 229–36.

Yang S. H. et al., *Pathological responses to oncogenic Hedgehog signalling in skin are dependent on canonical Wnt/ β -catenin signalling*, *Nat Genet.* 40, 1130-1135.

Zhao J. et al., *Tipping the balance: modulating the Wnt pathway for tissue repair*, *Trends in Biotechnology* 3, 131-136.

Giunta alla conclusione del mio lavoro, volevo dedicare un pensiero a chi ha reso possibile tutto questo...

Innanzitutto volevo ringraziare la professoressa Anna Maria Di Giulio che mi ha dato la possibilità di lavorare presso i suoi laboratori e far parte del suo gruppo di ricerca.

Un ringraziamento particolare al professor Alfredo Gorio per avermi sempre sostenuta, incoraggiata anche nei momenti di difficoltà e avermi dato l'occasione di dimostrare quanto valgo e di concludere questo lavoro.

A Stephana, non ci sono parole per ringraziarti. Grazie per la fiducia che mi hai dato nell'impostare e nello svolgere gli esperimenti; dell'importanza del ruolo affidatomi; per avermi aiutata nel lavoro e nello stendere questa tesi. Per essermi sempre stata vicina, per avermi sopportata (e so che non è facile....) per aver ascoltato tutti i miei problemi e avermi dato la possibilità di sfogarmi. Sai che sei stata la mia seconda mamma in questo periodo di permanenza a Milano.

Un grazie sincero a Giovanni, per avermi aperto gli occhi, per avermi fatto piangere e ridere e per essermi stato tanto vicino.

A Danka per tutti gli esperimenti che ha fatto per me quando non ne avevo voglia e per la sua amicizia sincera.

Un grazie particolare ad Andrea per aver donato i suoi 'pochi' bulbi rimasti al nostro esperimento e per la sua presenza nel nostro gruppo affiatato, così anche a Fanuel, nonostante sia appena arrivata, è stata fondamentale durante la stesura di questa tesi.

Alla mia cara amica Fra, la persona più simile e più diversa da me che abbia mai conosciuto, con la quale ho condiviso tutte le mie esperienze di questa vita milanese.

Ai miei fratelli che mi hanno fatto arrabbiare ma mi hanno voluto tanto bene. E io ne voglio tanto a voi!

Un grazie sentito a mia madre, senza la quale tutto questo non sarebbe stato possibile.

Ultima, ma non per importanza, grazie a te Cami, sei la cosa più bella della mia vita. Grazie per tutte le gioie che mi dai. Non immagini quanto io mi senta fortunata.